DNA-TR-85-214

THE IMPORTANCE OF SECONDARY ELECTRON COLLISIONAL IONIZATION (AVALANCHE) FOR X-RAY PULSES INCIDENT ON MISSILES-IN-FLIGHT

Howard W. Bloomberg
Beers Associates, Inc.
P. O. Box 2549
Reston, VA 22090-0549

14 May 1985

Technical Report

CONTRACT No. DNA 001-83-C-0036

Approved for public release;
distribution is unlimited.

THIS WORK WAS SPONSORED BY THE DEFENSE NUCLEAR AGENCY
UNDER RDT&E RMSS CODE B323085466 X99QMXVE00014 H2590D

Prepared for
Director
DEFENSE NUCLEAR AGENCY
Washington, DC 20305-1000

Destroy this report when it is no longer needed. Do not return to sender.

PLEASE NOTIFY THE DEFENSE NUCLEAR AGENCY, ATTN: STTI, WASHINGTON, DC 20305-1000, IF YOUR ADDRESS IS INCORRECT, IF YOU WISH IT DELETED FROM THE DISTRIBUTION LIST, OR IF THE ADDRESSEE IS NO LONGER EMPLOYED BY YOUR ORGANIZATION.

DISTRIBUTION LIST UPDATE

This mailer is provided to enable DNA to maintain current distribution lists for reports. We would appreciate your providing the requested information.

☐ Add the individual listed to your distribution list.

☐ Delete the cited organization/individual.

☐ Change of address.

NAME: _____

ORGANIZATION: _____

OLD ADDRESS	CURRENT ADDRESS
_____	_____
_____	_____
_____	_____

TELEPHONE NUMBER: ( ) _____

SUBJECT AREA(s) OF INTEREST:

_____	_____
_____	_____
_____	_____

DNA OR OTHER GOVERNMENT CONTRACT NUMBER: _____

CERTIFICATION OF NEED-TO-KNOW BY GOVERNMENT SPONSOR (if other than DNA):

SPONSORING ORGANIZATION: _____

CONTRACTING OFFICER OR REPRESENTATIVE: _____

SIGNATURE: _____

Director
Defense Nuclear Agency
ATTN: STTI
Washington, DC 20305-1000

Director
Defense Nuclear Agency
ATTN: STTI
Washington, DC 20305-1000

UNCLASSIFIED
SECURITY CLASSIFICATION OF THIS PAGE

AD-A168112

REPORT DOCUMENTATION PAGE

Form Approved
OMB No. 0704-0188
Exp. Date: Jun 30, 1986

1a. REPORT SECURITY CLASSIFICATION UNCLASSIFIED	1b. RESTRICTIVE MARKINGS
2a. SECURITY CLASSIFICATION AUTHORITY N/A since Unclassified	3. DISTRIBUTION/AVAILABILITY OF REPORT Approved for public release; distribution is unlimited.
2b. DECLASSIFICATION/DOWNGRADING SCHEDULE N/A since Unclassified	
4. PERFORMING ORGANIZATION REPORT NUMBER(S) BEERS-1-85-1010-53	5. MONITORING ORGANIZATION REPORT NUMBER(S) DNA-TR-85-214
6a. NAME OF PERFORMING ORGANIZATION Beers Associates, Inc. — 6b. OFFICE SYMBOL (If applicable)	7a. NAME OF MONITORING ORGANIZATION Director Defense Nuclear Agency
6c. ADDRESS (City, State, and ZIP Code) P.O. Box 2549 Reston, VA 22090-0549	7b. ADDRESS (City, State, and ZIP Code) Washington, DC 20305-1000
8a. NAME OF FUNDING/SPONSORING ORGANIZATION — 8b. OFFICE SYMBOL (If applicable)	9. PROCUREMENT INSTRUMENT IDENTIFICATION NUMBER DNA 001-83-C-0036
8c. ADDRESS (City, State, and ZIP Code)	10 SOURCE OF FUNDING NUMBERS PROGRAM ELEMENT NO.: 62715H; PROJECT NO.: X99QMXV; TASK NO.: E; WORK UNIT ACCESSION NO.: DH007959

11. TITLE (Include Security Classification)
THE IMPORTANCE OF SECONDARY ELECTRON COLLISIONAL IONIZATION (AVALANCHE) FOR X-RAY PULSES INCIDENT ON MISSILES-IN-FLIGHT

12. PERSONAL AUTHOR(S)
Bloomberg, Howard W.

13a. TYPE OF REPORT	13b. TIME COVERED	14. DATE OF REPORT (Year, Month, Day)	15. PAGE COUNT
Technical Report	FROM 840201 TO 850514	850514	52

16. SUPPLEMENTARY NOTATION
This work was sponsored by the Defense Nuclear Agency under RDT&E RMSS Code B323085466 X99QMXVE00014 H2590D.

17. COSATI CODES		
FIELD	GROUP	SUB-GROUP
20	8	
16	4	

18. SUBJECT TERMS (Continue on reverse if necessary and identify by block number)
Avalanche; Secondary Electrons; Ionization; Air Chemistry; X-Ray Pulse; Swarm Theory; Nuclear Weapons Effects; Monte Carlo technique;

19. ABSTRACT (Continue on reverse if necessary and identify by block number)
This report presents a series of contour plots for both strong and moderate avalanche on the electric field-pressure plane. Plots are given for effective electric field durations from 0.1 to 100 ns, consistent with times corresponding to X-ray pulse widths of interest in nuclear weapon effects. The computations were carried out with special concern for accuracy. The adequacy of the air chemistry data set is confirmed by comparison with experimental swarm data. The effect of the delay for the avalanche frequency to reach its steady state value is included in the calculations.

Keywords:
System Generated Electromagnetic Pulse (SGEMP);
Single Electron Monte Carlo (SEMC).

20. DISTRIBUTION/AVAILABILITY OF ABSTRACT	21 ABSTRACT SECURITY CLASSIFICATION
☐ UNCLASSIFIED/UNLIMITED ☒ SAME AS RPT ☐ DTIC USERS	UNCLASSIFIED
22a. NAME OF RESPONSIBLE INDIVIDUAL Betty L. Fox	22b. TELEPHONE (Include Area Code) (202) 325-7042 — 22c. OFFICE SYMBOL DNA/STTI

DD FORM 1473, 84 MAR — 83 APR edition may be used until exhausted. All other editions are obsolete.

SECURITY CLASSIFICATION OF THIS PAGE
UNCLASSIFIED

SUMMARY

Use of the Monte Carlo SEMC chemistry data package has authenticated its validity for the region $E/p < (E/p)_{cr}$ where the results were compared with steady state experimental data. The effects of finite delay on avalanche were examined for $E/p < (E/p)_{cr}$. It was found that neglect of this delay leads to overestimates of the avalanche up to a factor of about 2; the precise error depends on the time interval of interest and on the ratio E/p. Having proven the accuracy of the SEMC chemistry data set for the regime where experimental data is available, we believe that it is important to determine the effects of avalanche in the regime $E/p > (E/p)_{cr}$. Here no steady state exists and experimental data is not available. For finite time intervals, however, substantial avalanche can be expected. Evaluation of avalanche effects in this regime for the pulse widths of interest is an important next step.

The data from the Monte Carlo model reported by Bloomberg and Pine (1984) were displayed in a form useful for analysts who wish to check the importance of avalanche in their particle push algorithms. Contour plots for avalanche e-folding values of $\Gamma = 1$ and $\Gamma = 5$ are presented on the E-p plane for a given characteristic time. Alternatively, an expression for the e-folding value for particular E, p, and characteristic time, t_p, is given by Equation (5).

CONVERSION TABLE

Conversion factors for U.S. Customary to metric (SI) units of measurement

MULTIPLY → / TO GET ←	BY → / BY ←	TO GET → / DIVIDE ←
angstrom	1.000 000 X E -10	meters (m)
atmosphere (normal)	1.013 25 X E +2	kilo pascal (kPa)
bar	1.000 000 X E +2	kilo pascal (kPa)
barn	1.000 000 X E -28	meter^2 (m^2)
British thermal unit (thermochemical)	1.054 350 X E +3	joule (J)
calorie (thermochemical)	4.184 000	joule (J)
cal (thermochemical)/cm^2	4.184 000 X E -2	mega joule/m^2 (MJ/m^2)
curie	3.700 000 X E +1	*giga becquerel (GBq)
degree (angle)	1.745 329 X E -2	radian (rad)
degree Fahrenheit	t_K = (t° f + 459.67)/1.8	degree kelvin (K)
electron volt	1.602 19 X E -19	joule (J)
erg	1.000 000 X E -7	joule (J)
erg/second	1.000 000 X E -7	watt (W)
foot	3.048 000 X E -1	meter (m)
foot-pound-force	1.355 818	joule (J)
gallon (U.S. liquid)	3.785 412 X E -3	meter^3 (m^3)
inch	2.540 000 X E -2	meter (m)
jerk	1.000 000 X E +9	joule (J)
joule/kilogram (J/kg) (radiation dose absorbed)	1.000 000	Gray (Gy)
kilotons	4.183	terajoules
kip (1000 lbf)	4.448 222 X E +3	newton (N)
kip/inch^2 (ksi)	6.894 757 X E +3	kilo pascal (kPa)
ktap	1.000 000 X E +2	newton-second/m^2 (N-s/m^2)
micron	1 000 000 X E -6	meter (m)
mil	2.540 000 X E -5	meter (m)
mile (international)	1.609 344 X E +3	meter (m)
ounce	2.834 952 X E -2	kilogram (kg)
pound-force (lbs avoirdupois)	4.448 222	newton (N)
pound-force inch	1.129 848 X E -1	newton-meter (N·m)
pound-force/inch	1.751 268 X E +2	newton/meter (N/m)
pound-force/foot^2	4.788 026 X E -2	kilo pascal (kPa)
pound-force/inch^2 (psi)	6.894 757	kilo pascal (kPa)
pound-mass (lbm avoirdupois)	4.535 924 X E -1	kilogram (kg)
pound-mass-foot^2 (moment of inertia)	4.214 011 X E -2	kilogram-meter^2 (kg·m^2)
pound-mass/foot^3	1.601 846 X E +1	kilogram/meter^3 (kg/m^3)
rad (radiation dose absorbed)	1.000 000 X E -2	**Gray (Gy)
roentgen	2.579 760 X E -4	coulomb/kilogram (C/kg)
shake	1.000 000 X E -8	second (s)
slug	1.459 390 X E +1	kilogram (kg)
torr (mm Hg, 0° C)	1.333 22 X E -1	kilo pascal (kPa)

*The becquerel (Bq) is the SI unit of radioactivity; 1 Bq = 1 event/s.
**The Gray (Gy) is the SI unit of absorbed radiation.

TABLE OF CONTENTS

LIST OF ILLUSTRATIONS

SECTION 1

INTRODUCTION

It has become clear that techniques used by the SGEMP community to predict responses in tests simulating X-rays incidents on missiles-in-flight are inadequate. A major reason for this lack of fidelity would seem to be associated with the absence of important air chemistry in algorithms describing secondary electrons as well as energetic phtotelectrons. A demonstrably satisfactory air chemistry data set has recently been collected and used to compute secondary electron transport in a Monte Carlo algorithm SEMC (Bloomberg and Pine, 1984). In this report we apply results from Bloomberg and Pine (1984) to quantify the effects of secondary electron collisional ionization (avalanche) over the short time intervals of interest in the study of X-ray pulse phenomena.

It is interesting to consider why the community has so long eschewed the incorporation of systematic air chemistry data into the algorithms used to predict responses for missile-in-flight test simulations. The reason is that complete air chemistry data is relatively unimportant when describing secondary effects in the very low and very high pressure regimes. In the low pressure regimes secondaries are accelerated rapidly to high energies. At high energies the electron neutral particle interactions are relatively simple. Large angle elastic scattering is unimportant and the energy losses to inelastic processes are small. On the other hand, at high pressure the associated air chemistry is complicated. Since electron distributions quickly establish steady states, however, details of the air chemistry are not important in the determination of electron transport. Adequate empirical swarm data exist in this regime to characterize the required electron transport.

It is clear from the above discussion that detailed knowledge of air chemistry is required in order to characterize the intermediate pressure regime. The implied hope of the community that the effective intermediate pressure regime would be sufficiently narrow so as not to affect the

phenomenology seems not to have been realized. Indeed, it is acknowledged that important phenomena may occur just in the intermediate pressure regime. Accordingly, many experiments have been conducted at pressures wherre existing models are known to be inaccurate. The work of Bloomberg and Pine (1984) incorporated a thorough chemistry data set for nitrogen. A Monte Carlo model was used to obtain the time dependent electron distribution. The transient transport coefficients were obtained by appropriate particle scoring. The problem was restricted to the case of spatially uniform distributions. Moreover, the electric field was a specified fixed value throughout space and time. Under these conditions the model allows a consistent evaluation of electron transport coefficients over the entire range of pressures.

This report begins to delineate the characteristics of the important intermediate pressure regime for X-ray pulses incident on missiles-in-flight. We concentrate our attention on the ionization coefficient or, alternatively, the collisional ionization frequency for secondary electrons. In Section 2 we distinquish the cases where secondaries in a constant electric field can either approach a steady state or a runaway condition. In Section 3 we examine the regime for which steady-state transport is possible. We argue that there is a delay time required to set up the steady-state distribution. For finite X-ray pulse durations this delay can change the avalanche effect as compared to when steady values are used over the entire pulse. The effects are put in quantitive terms. In Section 4 we discuss the ramifications of the work on X-ray simulations of missile-in-flight environments. In particular, we argue that the effective pulse width is an important parameter in the representation of the intermediate pressure regime. The results are discussed and summarized in Sections 5 and 6, respectively. Appendix A contains mathematical details used to obtain the results; Appendix B contains the background paper of Bloomberg and Pine (1984).

SECTION 2

STEADY-STATE TRANSPORT AND SECONDARY RUNAWAY

It is important for us to characterize the division between the high pressure regime, where steady state obtains and the low pressure regime, where the electric field continuously accelerates the secondary electrons. The equation of motion for a single electron is given by

$$m_e \frac{dv}{dt} + m_e \nu_m v = eE \qquad (1)$$

Where ν_m is the momentum transfer frequency, that is the frequency for large angle elastic scatter

$$\nu_m = \sigma_m v n_b \qquad (2)$$

where σ_m is the energy dependent momentum transfer cross section, v is the electron velocity, and n_b is the density of the background neutral particles. The largest possible value of the drag term in Equation (1) is

$$m_e n_b \, \mathrm{Max}\{\sigma_m v^2\}$$

It is reasonable to assume that whenever the electric field exceeds this maximum drag that electrons will run away, i.e., continually gain more energy from the electric field than is lost through collisions. The critical field so defined is directly proportional to the background number density. It is convenient, therefore, to define a critical ratio of the field strength to the background number density or, alternatively, the field to pressure ratio. For an N_2 background the computed critical ratio is

$$(E/p)_{cr} = 1.4 \cdot 10^5 \, V/(m \cdot Torr) \qquad (3)$$

Swarm data traditionally are plotted against E/p as the independent parameter. Since the data are steady state it follows that swarm theory holds only for those parameters smaller than the critical value of Equation (3).

SECTION 3

TRANSIENT BEHAVIOR

The guiding principle in the work of Bloomberg and Pine (1984) is to include sufficient chemistry de-excitation as well as elastic and collisional ionization processes, so that experimental swarm data could be approximated in the time asymptotic limit. A measure of the success of this program is shown in Figure 1. Here the ionization rates were scored over the time histories tracked in the Monte Carlo procedure. The X's show the numerical results in the long time limits for various values of the parameter E/p. The solid line in Figure 1 shows ionization coefficients from the experimental swarm data collected by Dutton (1975). The agreement with experiment is good, and this is verification that the chemistry incorporated in the Monte Carlo algorithm is sufficiently complete and accurate to treat the time-dependent electron transport problem. There is a discrepancy between the calculated and experimentally determined ionization coefficients at $E/p \sim 7 \cdot 10^{5}$ $V \cdot m^{-1} \cdot Torr^{-1}$. This may indicate that the critical ratio of E/p is somewhat lower than we have estimated, and that steady state is not being achieved at the upper end of the curve in Figure 1. It must be emphasized that the agreement between calculation and experiment in Figure 1 gives us confidence in using the Monte Carlo algorithm over all values of E/p. For values above the critical ratio there will be no steady state, but the resulting transient solutions should give the correct behavior.

We now direct our attention to the transient behavior of the frequency of collisional ionization due to secondaries for values of $E/p < (E/p)_{cr}$, i.e., when steady state is achieved. At their moment of creation secondary electrons (the so-called source electrons) have low energies. In the presence of an electric field source electrons are first accelerated. Eventually the increase in electron energy from the field is balanced by losses through collisions with the background neutral particles. Similarly, a momentum balance is achieved. Obviously there is a delay in achieving the steady state values. This is shown in Figure 2, where the ionization coefficient, α, a

measure of the spatial avalanche growth, and the drift velocity are plotted as functions of time. Note that the delay for the avalanche coefficient is much greater than for the drift velocity. This is to be expected since the drift velocity is a measure of the bulk electron distribution, whereas the ionization coefficient depends on the distribution of electrons with energies large enough to cause ionization (>15.6 eV in N_2). It clearly takes longer for the wings of the distribution to establish their steady state.

Collisional ionization by secondaries is one of the most important processes for the understanding of missile-in-flight phenomena. The finite time delay in reaching steady state means that use of the steady stae ionization frequency over the entire pulse width overestimates the avalanche. To determine the effect of delay we prescribe the time dependence of the ionization frequency by function

$$\nu = \bar{\nu} \left[1 - \exp\left(-t/t_d\right)\right] \tag{4}$$

where t_d is the decay time determined from best fits to the Monte Carlo results; $\bar{\nu}$ is the steady state value. We show in Appendix A that the product pt_d is itself a function only of E/p. The functional dependence has been determine. from Monte Carlo runs where the value of t_d was obtained from fits to the numerical data. The resulting plot is shown in Figure 3. Note that for a given p, t_d decreases with increasing E. This result is expected since the higher field acceleration should diminish the time required for initially stationary secondary electrons to achieve their steady-state distribution. The pressure normalized steady-state collision frequency is also only a function of E/p. The functional form can be recovered from the Dutton (1975) data and is shown in Figure 4. This completes specification of the time dependent ionization frequency for values of E/p small enough so that a steady state value eventually is achieved, as implied in Equation (4).

SECTION 4

RESULTS

We now discuss the effects of non-zero time delays over finite pulse widths t_d. All thin air SGEMP processes are limited to finite time intervals. The interval of concern here is that for which the electric field strength remains relatively constant. This duration is difficult to determine, because it is affected in part by self-consistent effects from the very ionization phenomena we are attempting to describe. Nevertheless, it is useful in this analysis to introduce an effective time interval. In general, the time of interest can be associated simply with the X-ray radiation pulse width.

The importance of incorporating finite delay time into calculations depends on the time interval t_d. It is obvious from Equation (4) that neglect of the delay time overestimates the number of ionizations in any given time interval. The magnitude of the overestimating error resulting from use only of the steady-state ionization frequency over the time interval has been calculated. Details of the calculation are presented in Appendix A, and the results are plotted in Figure 5. Here the overestimate factor for several values of the parameter pt_p is plotted as a function of E/p. For small pt_p the overestimate factor is close to unity over the range of E/p under consideration. This is simply a manifestation of the fact that the time interval is so small that hardly any collisional ionizations result from a secondary electron. Thus the delay time has little effect, since ionization is unimportant over the time interval even when the steady-state value is used. For larger pt_p neglect of the delay time leads to a more significant error. Finally, for very large pt_p the overestimate factor reaches a limit for a given value of E/p. This limit is easily understood. For $t>>t_d$ the actual ionization rate is nearly the steady-state value. Thus, increasing the value of t_p when $t_p>>t_d$ will not lead to additional increases in the overestimate.

It is interesting to note that the overestimate does not exceed a value of about 2, which occurs for large E/p. The reason for this is that while the ionization frequency becomes important for large E/p, the delay time decreases for large E/p, so that the importance of delay is reduced. The net effect is that the overestimate is limited to a rather modest value. A more detailed discussion of this result is given in Appendix A.

Having shown that consideration of the delay time is important in the calculation of the number of secondary collisional ionization events over a pulse interval, t_p, we now address the larger question of when secondary collisonal ionization is an important effect. Collisional ionization is an important effect whenever the corresponding e-fold $\int_o^{tp} \nu dt = \Gamma \geq 1$, where ν is given by Equation (4).

In Appendix A we show that for any selected e-fold Γ a curve in $E/p - pt_p$ space is defined. In Figure 6 we present two curves for both a modest e-fold (Γ=1) and a large e-fold (Γ=5) for collisional ionization. In order to get a particular avalanche multiplication over the time interval for smaller pt_p the value of E/p must increase. For convenience consider p fixed; then as t_p decreases a larger avalanche rate is required to give the same multiplication. As E gets to be too large a runaway condition applies, and we no longer can apply the present theory. On the other hand, for very large t_p a smaller avalanche rate is required for the same multiplication. The value of E does not decrease indefinitely, however, since there is a critical value of E/p below which there is a zero avalanche rate.

We have unfolded the results of Figure 6 in Figure 7a-j to give e-fold contour plots for Γ=1 and Γ=5 onto the E-plane for fixed values of t_p. This format is a useful one to check the validity of the treatment of secondary collisional ionization in the numerical algorithms used for this air SGEMP predictions. For these predictions the pressure is specified. The codes themselves indicate the E field strengths and durations. Thus, the adequacy of air chemistry data in the predictive codes can be checked straightforwardly.

Let us now discuss the contour plots in the E-plane when we fix the pulse t_p. Note as we increase p the required value of E increases. The universal plot of Figure 6 indicates that on a given e-fold contour the ratio E/p decreases for increasing p. This implies that the increase in the required E with p is sub-linear, and this conforms with the plots on Figures 7a-j. For large enough p the required value of E increases most rapidly (nearly linearly with p). This occurs because, while the avalanche rate required for a given multiplication does not change, the ratio ν/p decreases with increasing p. For small enough ν/p the corresponding value E/p is essentially constant, so that E increases nearly linearly with increasing p.

In summary, Figures 7a-j give an indication (for a given characteristic time and pressure) the extent to which a given E-field can lead to significant collisional ionization by secondary electrons. It may be useful to compare quantitatively the secondary collisional ionization from self-consistent thin air SGEMP predictive codes with the results of this work. For this reason we reference (from Appendix A) the expressions for the growth factor of a single initiatory secondary electron.

The growth or multiplication factor is $G = \exp(\Gamma)$ where Γ is the e-fold defined by

$$\Gamma = g(E/p)\,[pt_p + f(E/p)\exp\{-pt_p/f(E/p)\} - f(E/p)] \qquad (5a)$$

where

$$f(E/p) \equiv pt_d \qquad (5b)$$

and

$$g(E/p) \equiv \bar{\nu}/p \qquad (5c)$$

are plotted in Figures 3 and 4, respectively.

SECTION 5

DISCUSSION OF RESULTS

Determination of the importance of avalanche in thin-air SGEMP requires information about the electric field strength throughout the air around missile surfaces. The electric field has not been a parameter of physical concern in most past analyses of thin-air SGEMP phenomena. Rather a greater emphasis has been placed on the determination through theory and experiment of the voltages at various missile surfaces. As mentioned before, the emphasis on differential voltages has been motivated by the belief in the community that the net flow of primary photoelectrons from one section of the missile to another is the most important thin-air phenomenon. In addition to stressing the importance of the electric field, we have also stressed the role of the characteristic time interval for the field. It is this quantity (or more generally the product, pt_d) that determines the importance of the delay time in the computation of the collisonal ionization frequency.

The issue of the duration of the effective time interval for the electric field is complex but important. There are two aspects to the problem. The first is structural and concerns how various parts of a modeled system connect with each other electrically. The second concerns air itself where there is another relaxation channel due to the number of secondary charge carriers. This is determined by the number of initiating electrons as well as by avalanche itself. In air directly exposed to incident X-rays the creation of electrons through photoemission or by collisional ionization of photoelectrons emitted from surfaces may be very large. In such cases the air conductivity might be sufficiently large so as to rapidly reduce field strengths through relaxation. Then there might be insufficient time for significant avalanche to occur. Another possibility is that only a moderate number of initiating secondary electrons are produced in air. This could happen if shadowing is important. The conductivity due to the initiating electrons would be relatively small so that the field strengths could be maintained for long times. Under these circumstances avalanche could become important.

The present work extends naturally to include causes for $E/p > (E/p)_{cr}$. In this regime there is no steady state, and, after long times, the collisonal ionization frequency decreases monotonically with increasing time. Over the finite time intervals of interest, however, the total avalanche for $E/p > (E/p)_{cr}$ may be substantial.

SECTION 6

LIST OF REFERENCES

1. Bloomberg, Howard W. and Vernon W. Pine, Thermalization of secondary electrons under AMSGEMP conditions, IEEE Trans. Nucl. Sci. (1984 Annual Conference on Nuclear and Space Radiation Effects), NS-3 (6), December 1984.

2. Dutton, J., A survey of swarm data, J. Phys. and Chem. Ref. Data, 4, p. 577, 1975.

The solid curve shows experimental data assembled by Dutton (1975).
The corresponding values obtained in this work are shown by the X's.

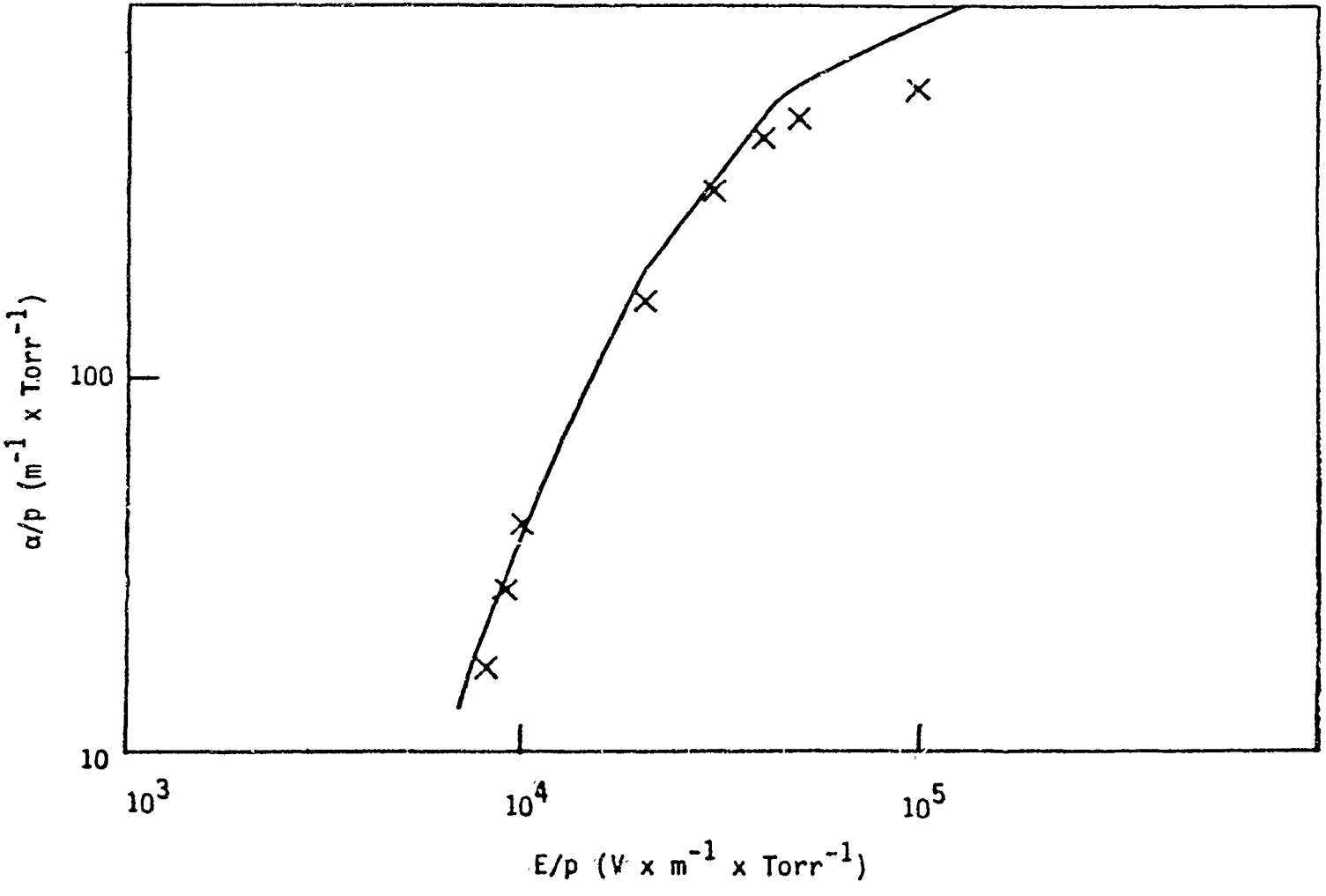

Figure 1. Steady-state ionization coefficient vs E/p.

Parameters are $E = 2 \cdot 10^4\ V \cdot M^{-1}$, p = 1 Torr.

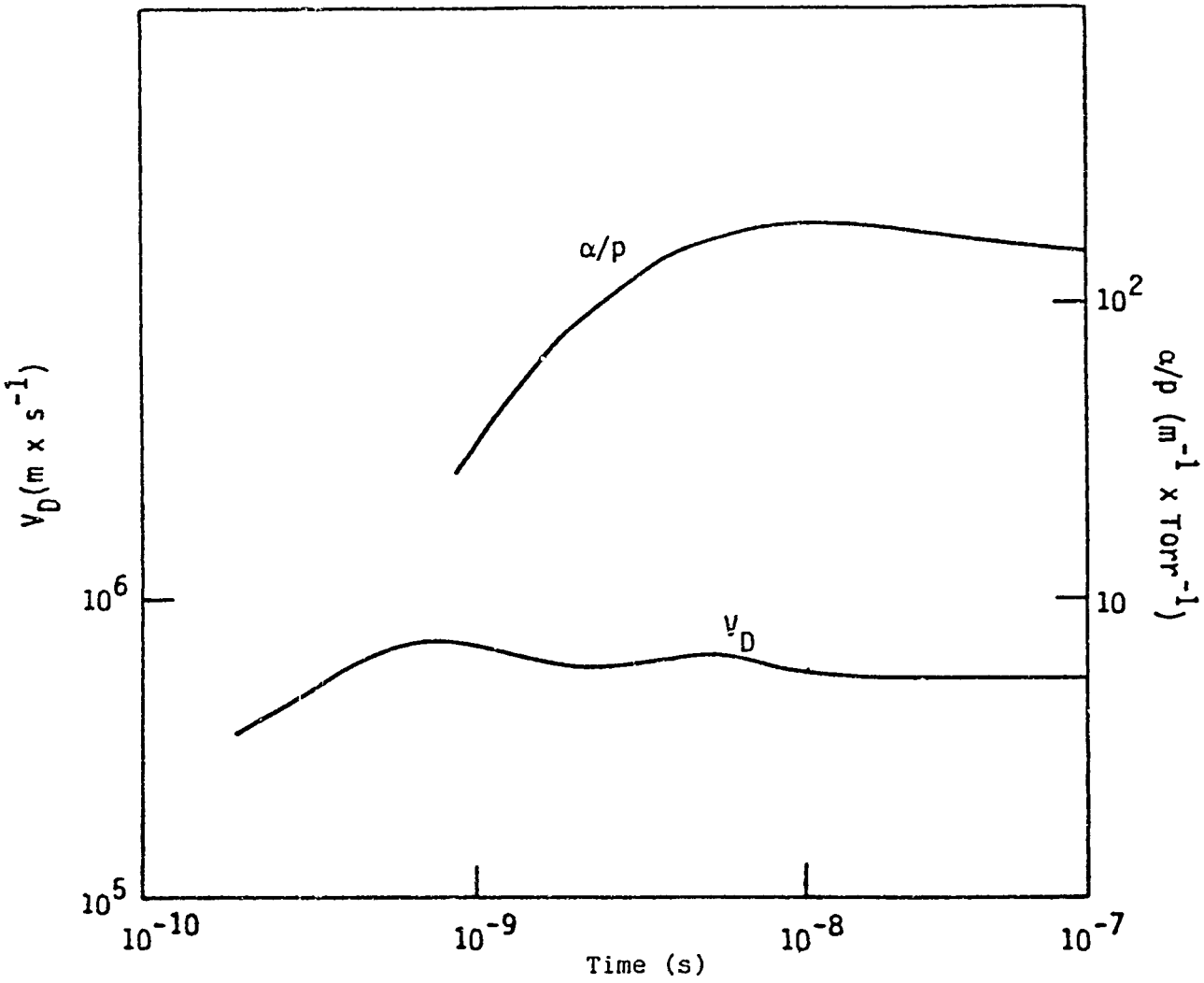

Figure 2. Drift velocity and coefficient as functions of time.

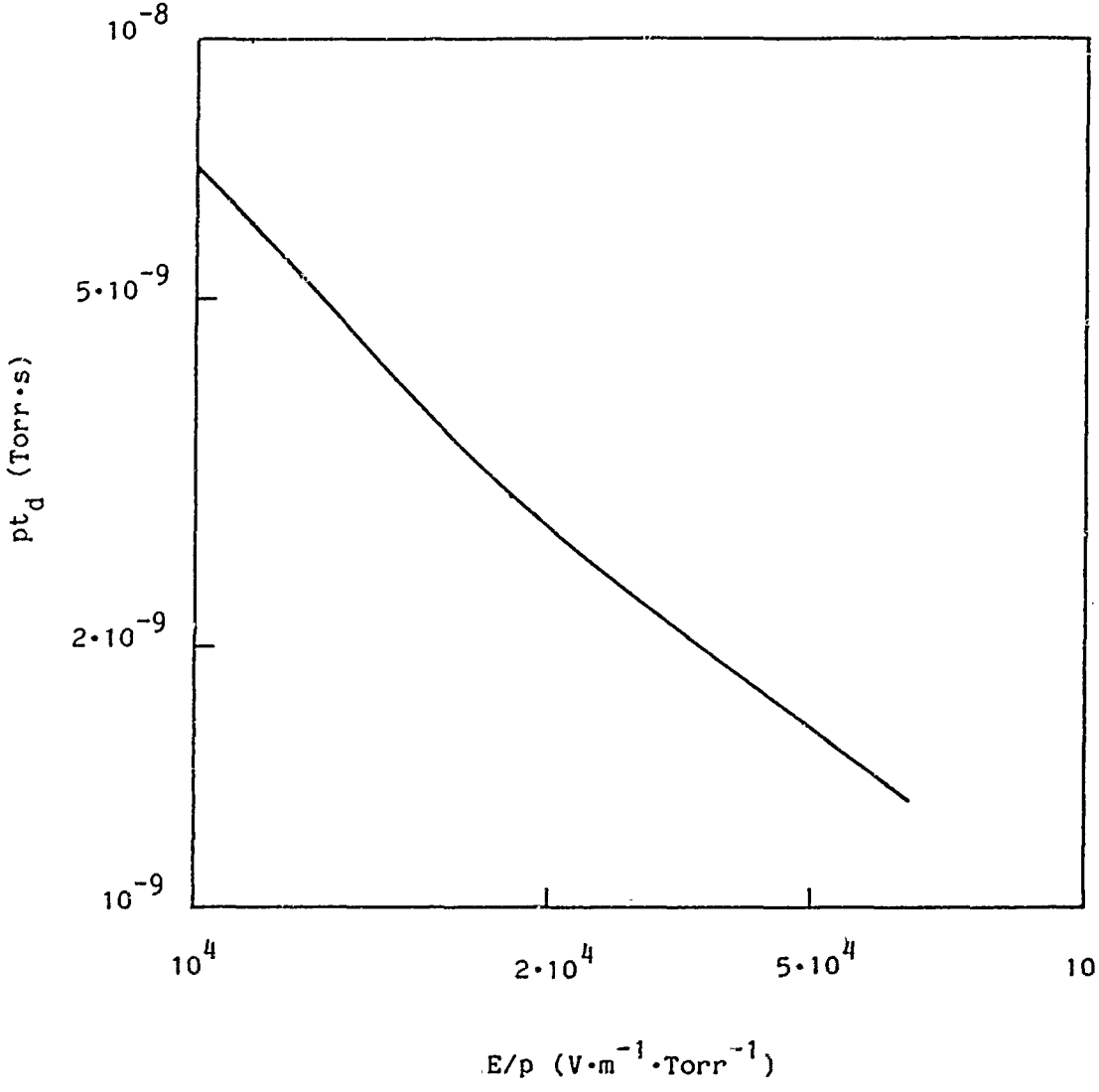

Figure 3. The product of pressure and decay time plotted as a function of E/p.

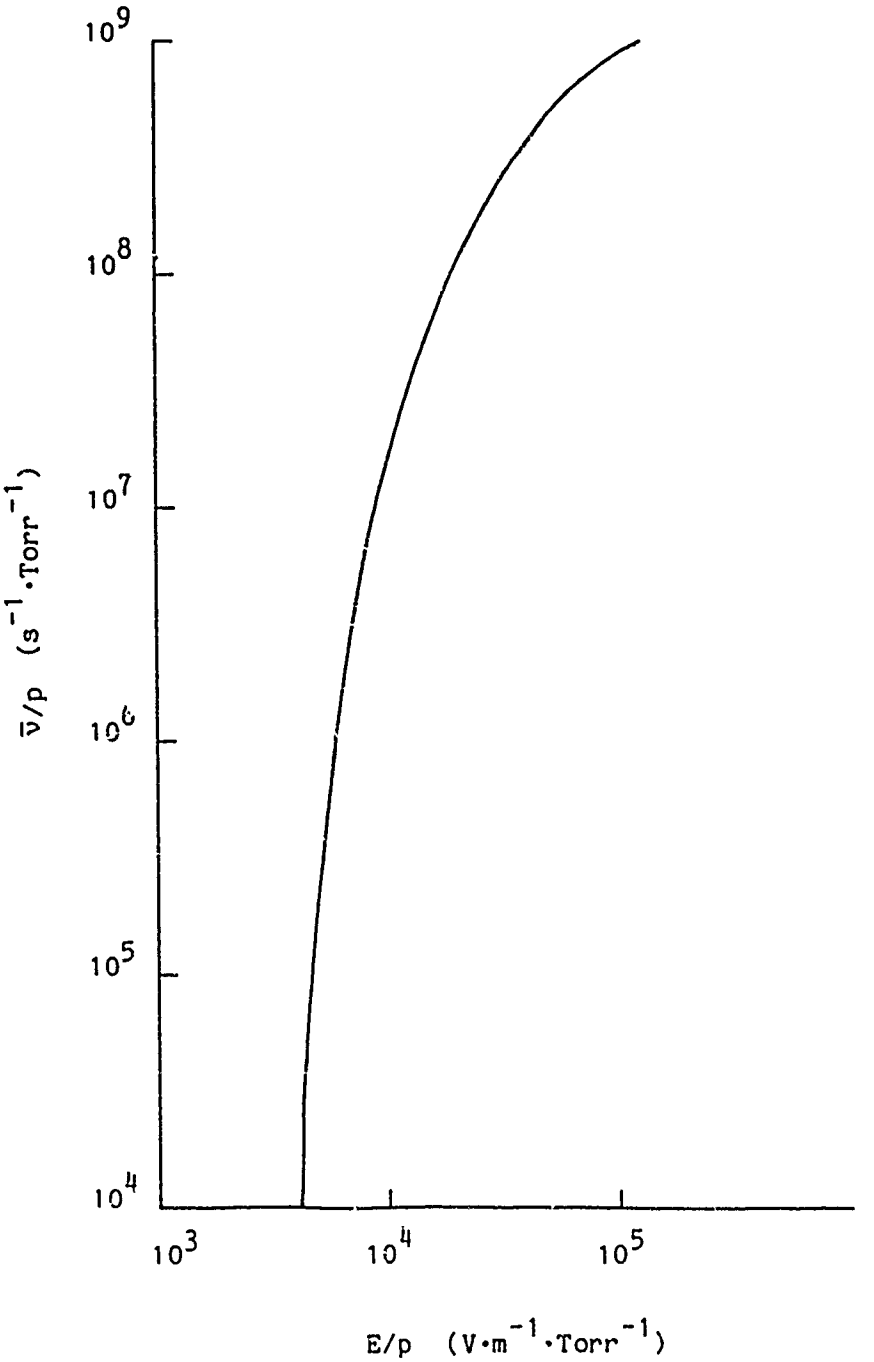

Figure 4. The pressure normalized steady-state collisional ionization frequency plotted as a function of E/p.

These plots show the error in the number of ionizations occurring in a pulse interval, t_p, in seconds when the ionization time delay is neglected.

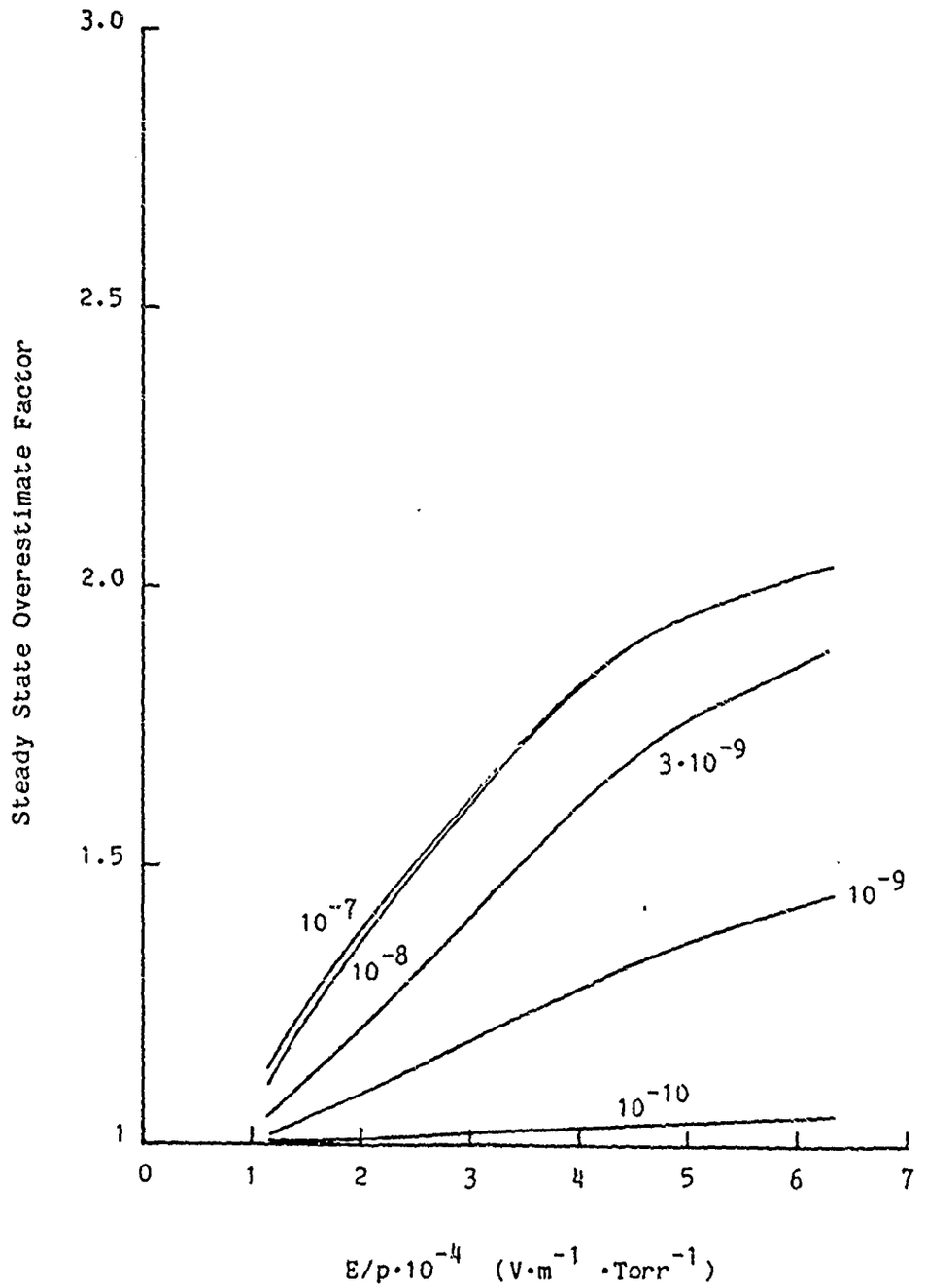

Figure 5. Steady-state overestimate factor.

Plotted are the contours for e-fold values $\Gamma = 1$ (corresponding to an ionization growth factor of 2.7) and $\Gamma = 5$ (corresponding to an ionization growth factor of 148).

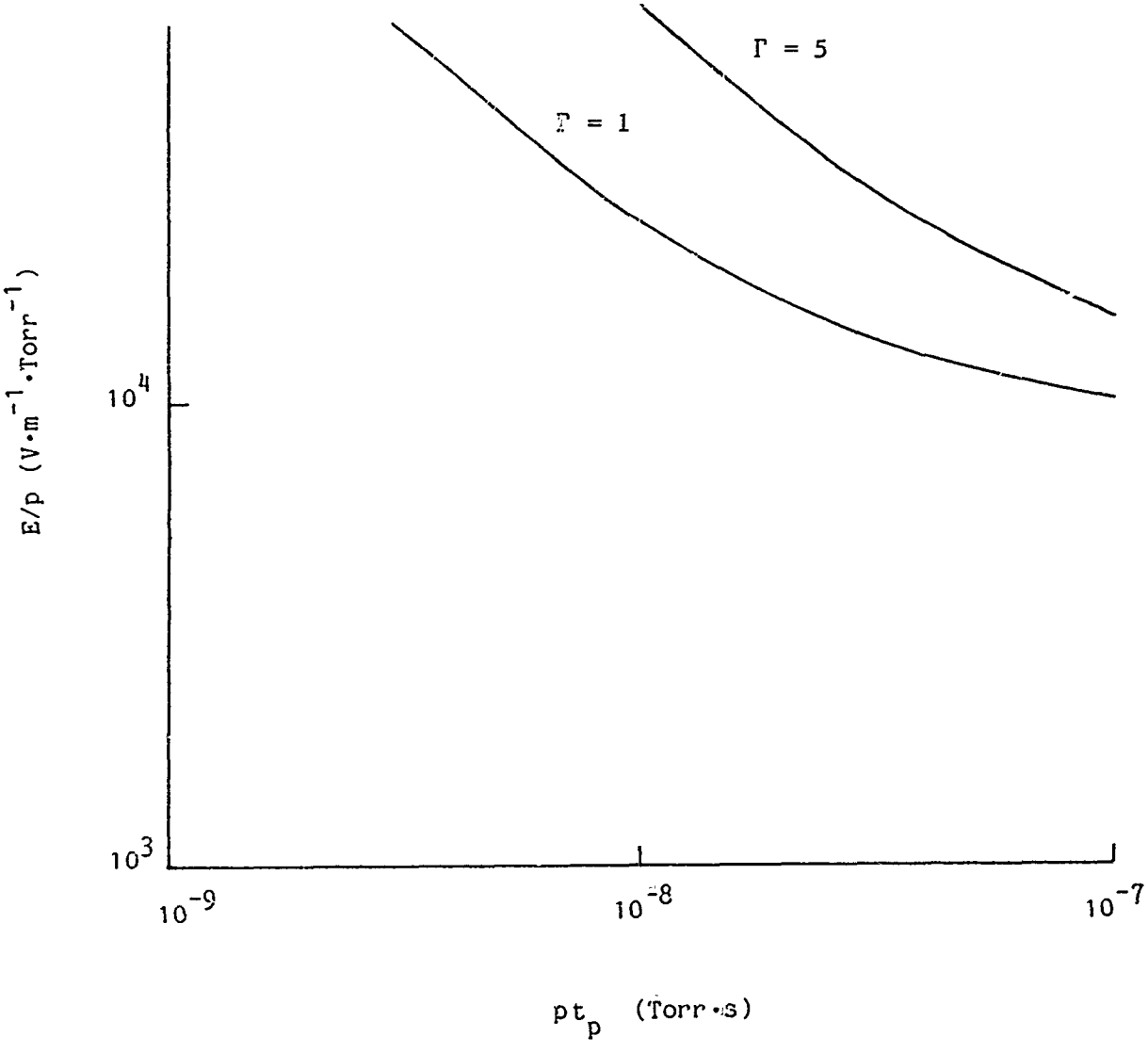

Figure 6. Contours for particular collisional ionization e-folding in the E/p - pt_p plane.

Plots derived from Figure 6 to show contours for the e-fold levels $\Gamma = 1$ and $\Gamma = 5$ in the E-p plane for various puls widths t_p:

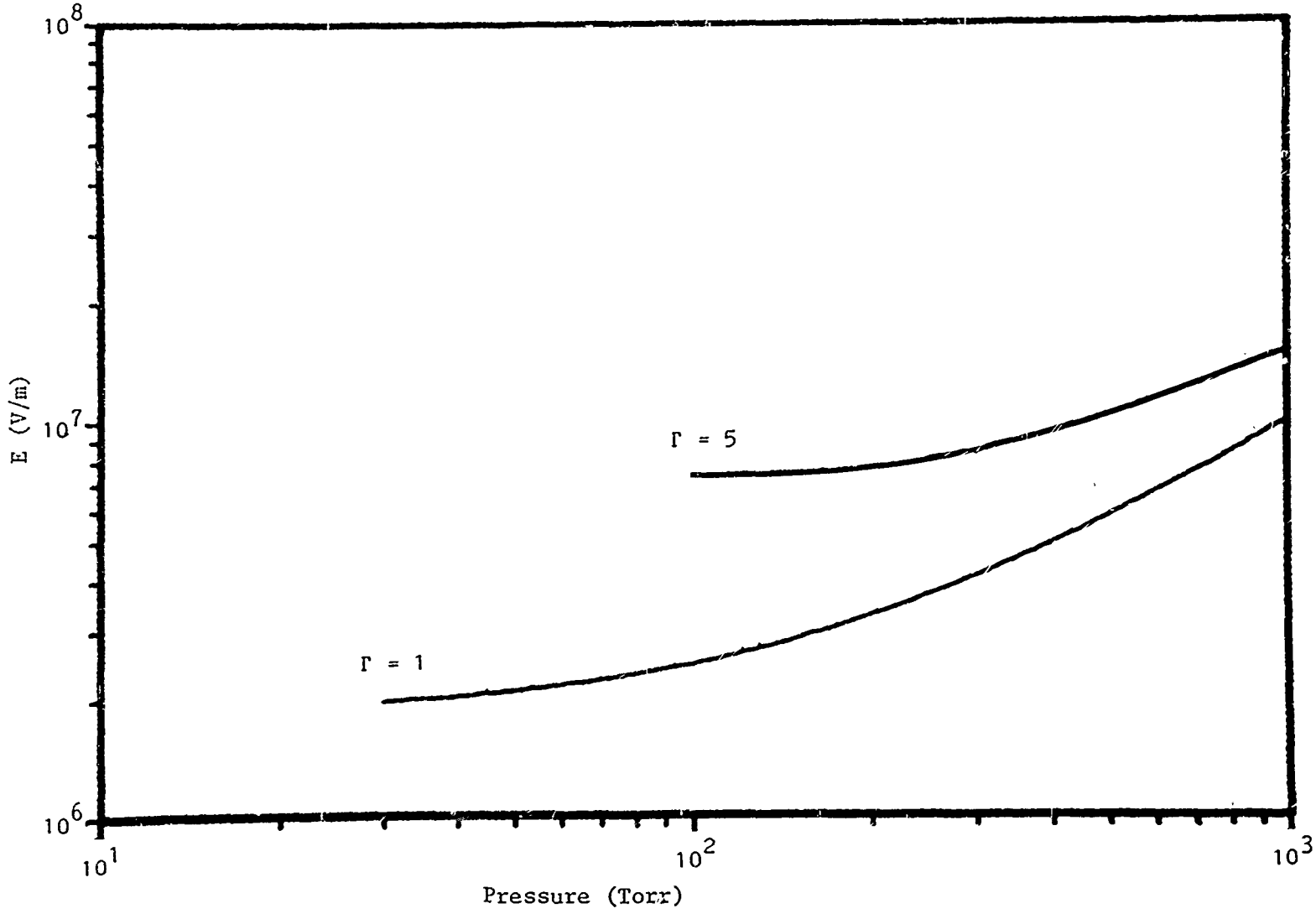

Figure 7a. (t(p) = 10E-10) sec.

Plots derived from Figure 6 to show contours for the e-fold levels $\Gamma = 1$ and $\Gamma = 5$ in the E-p plane for various pulse widths t_p:

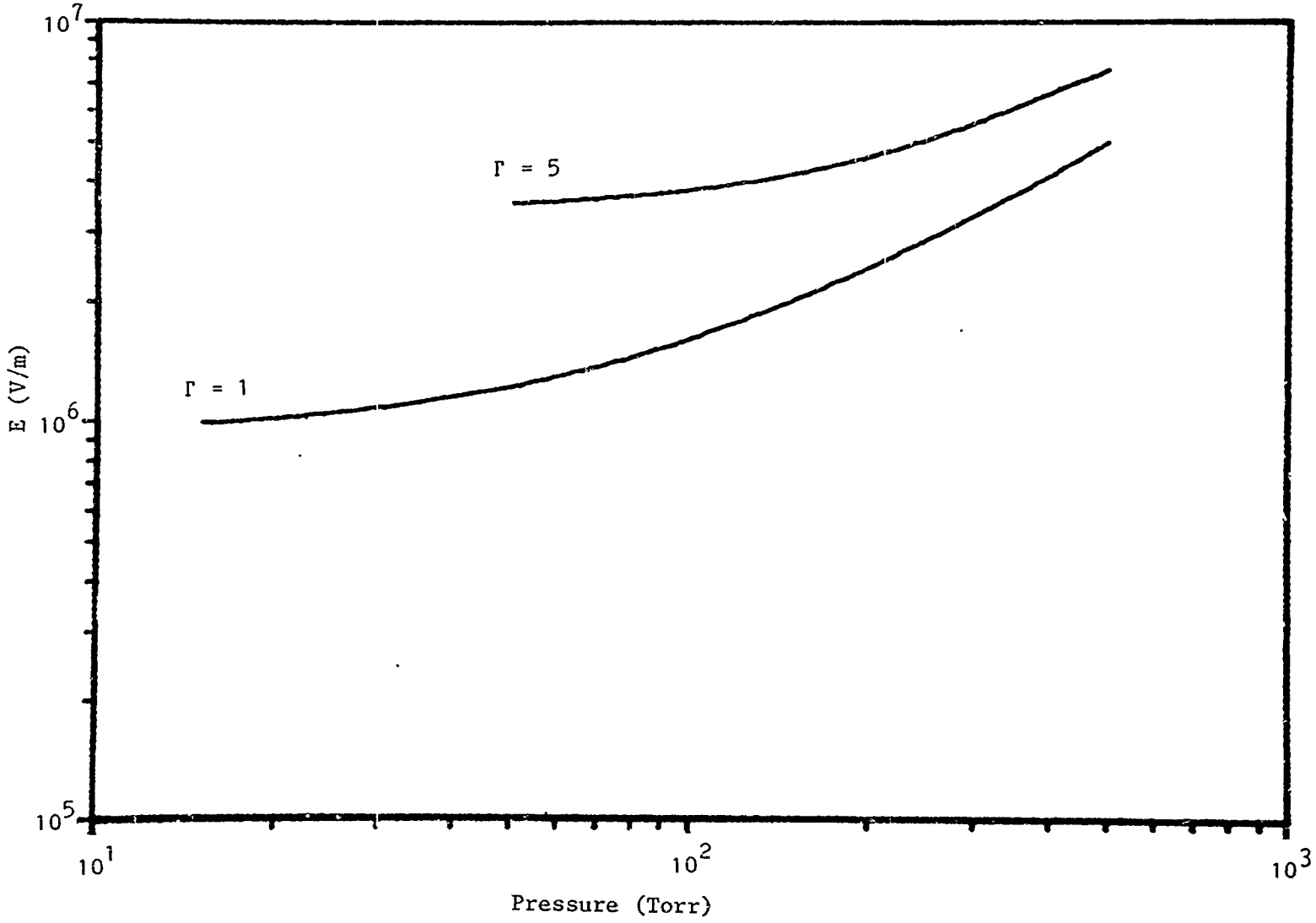

Figure 7b. (t(p) = 2x10E-10) sec.

Plots derived from Figure 6 to show contours for the e-fold levels $\Gamma = 1$ and $\Gamma = 5$ in the E-p plane for various pulse widths t_p:

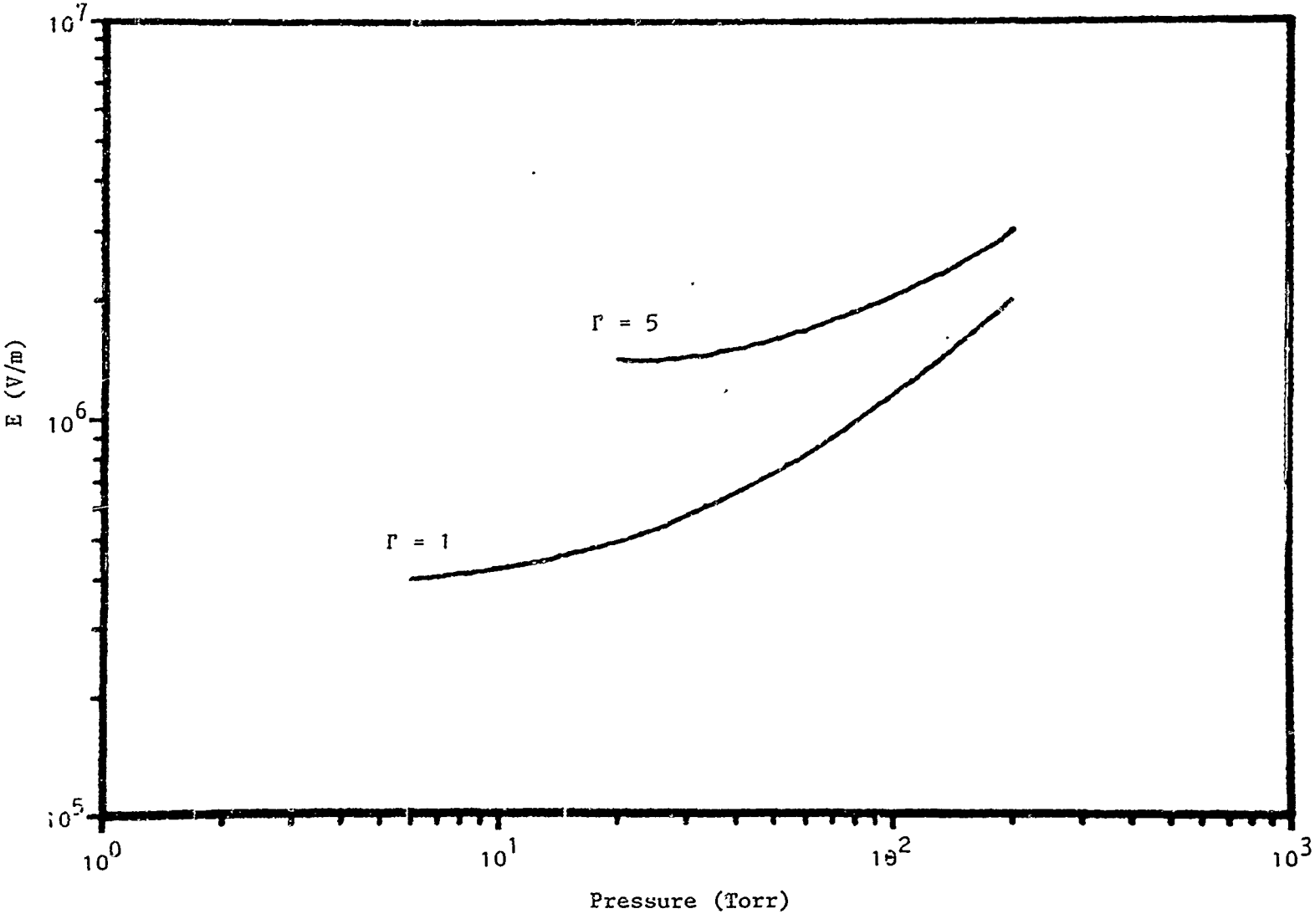

Figure 7c. (t(P) = 5x10E-10) sec.

Plots derived from Figure 6 to show contours for the e-fold levels $\Gamma = 1$ and $\Gamma = 5$ in the E-p plane for various pulse widths t_p:

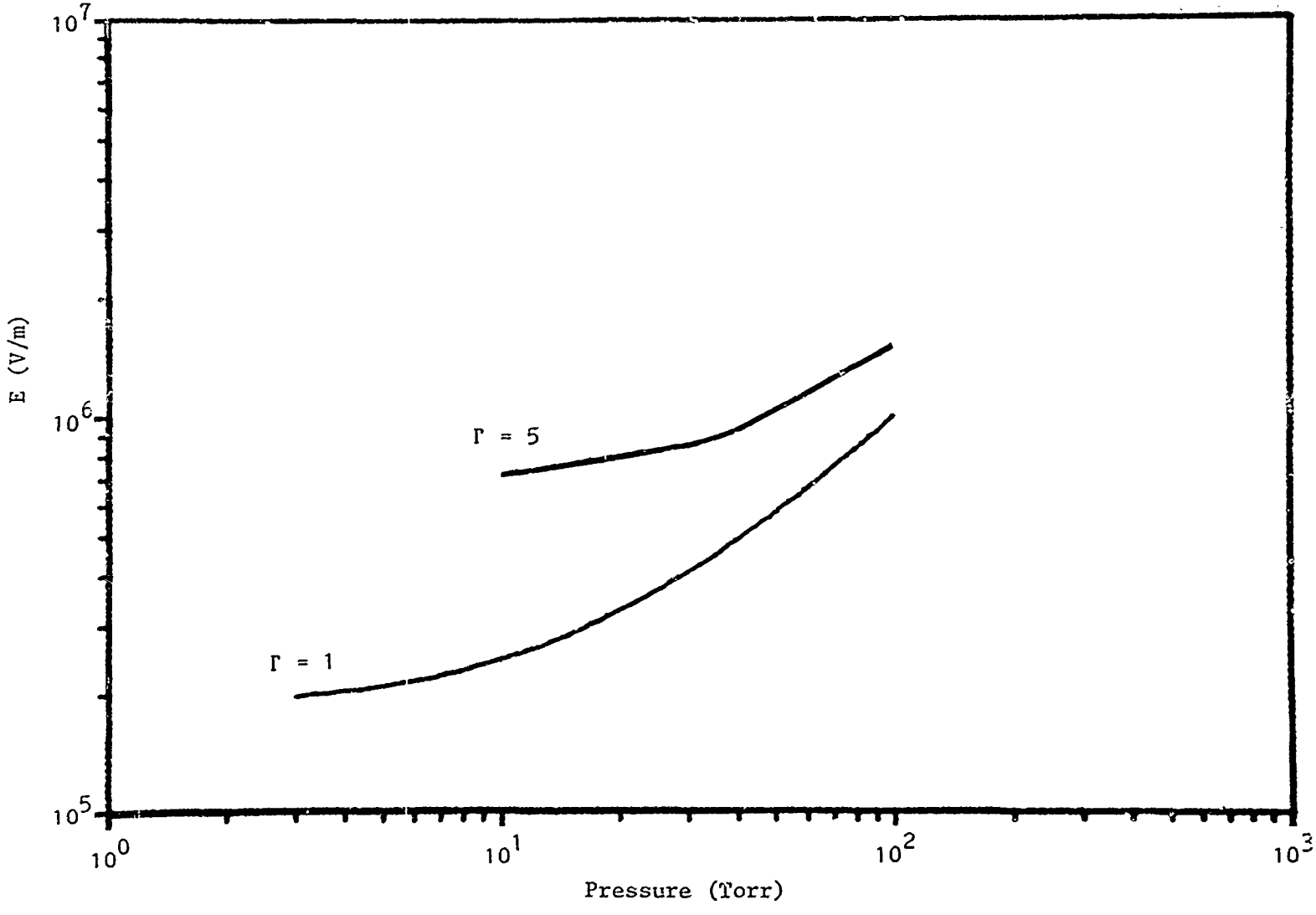

Figure 7d. (t(p) = 10E-9) sec.

Plots derived from Figure 6 to show contours for the e-fold levels $\Gamma = 1$ and $\Gamma = 5$ in the E-p plane for various pulse widths t_p:

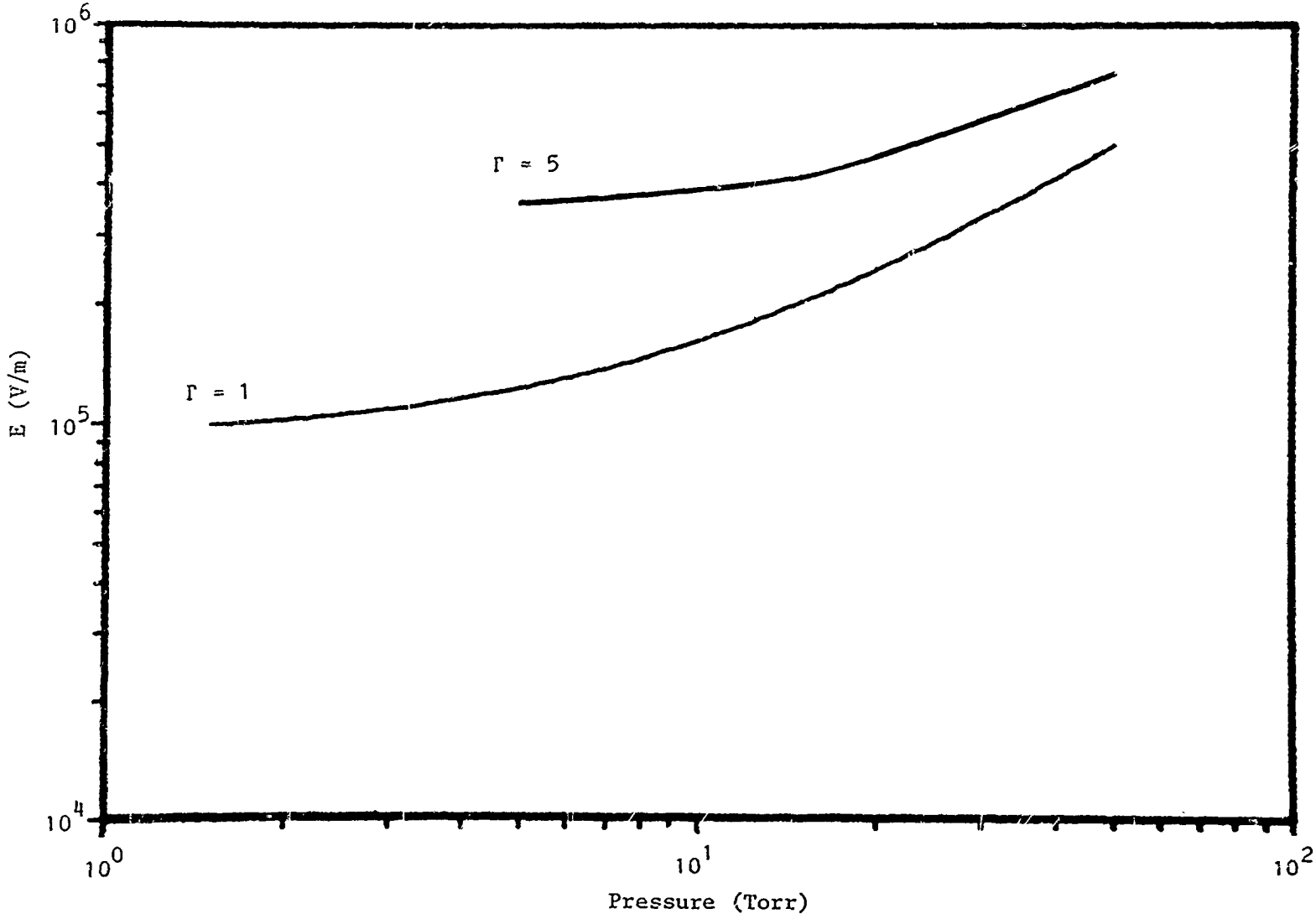

Figure 7e. (t(p) = 2x10E-9) sec.

Plots derived from Figure 6 to show contours for the e-fold levels $\Gamma = 1$ and $\Gamma = 5$ in the E-p plane for various pulse widths t_p:

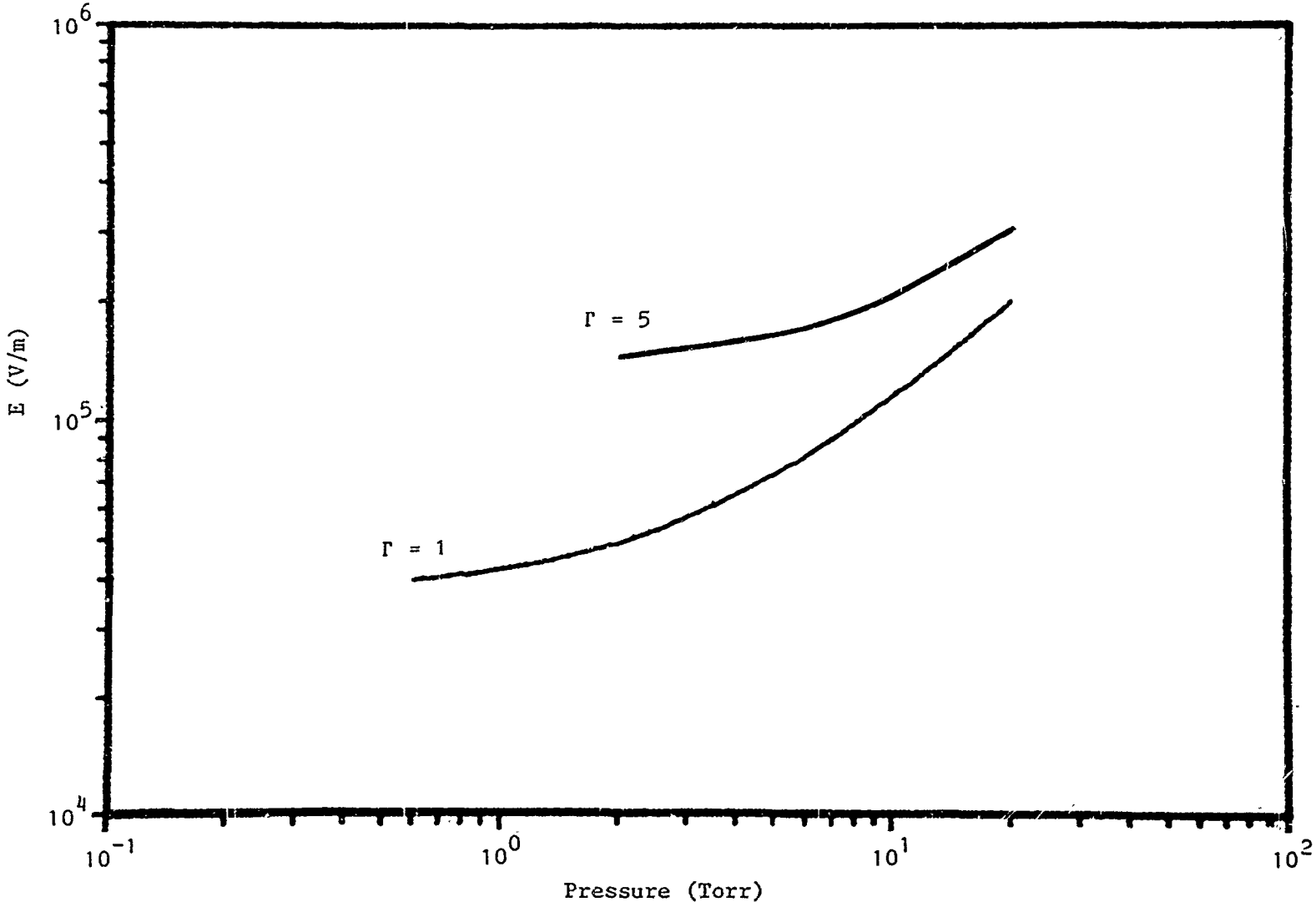

Figure 7f. (t(p) = 5x10E-9) sec.

Plots derived from Figure 6 to show contours for the e-fold levels $\Gamma = 1$ and $\Gamma = 5$ in the E-p plane for various pulse widths t_p:

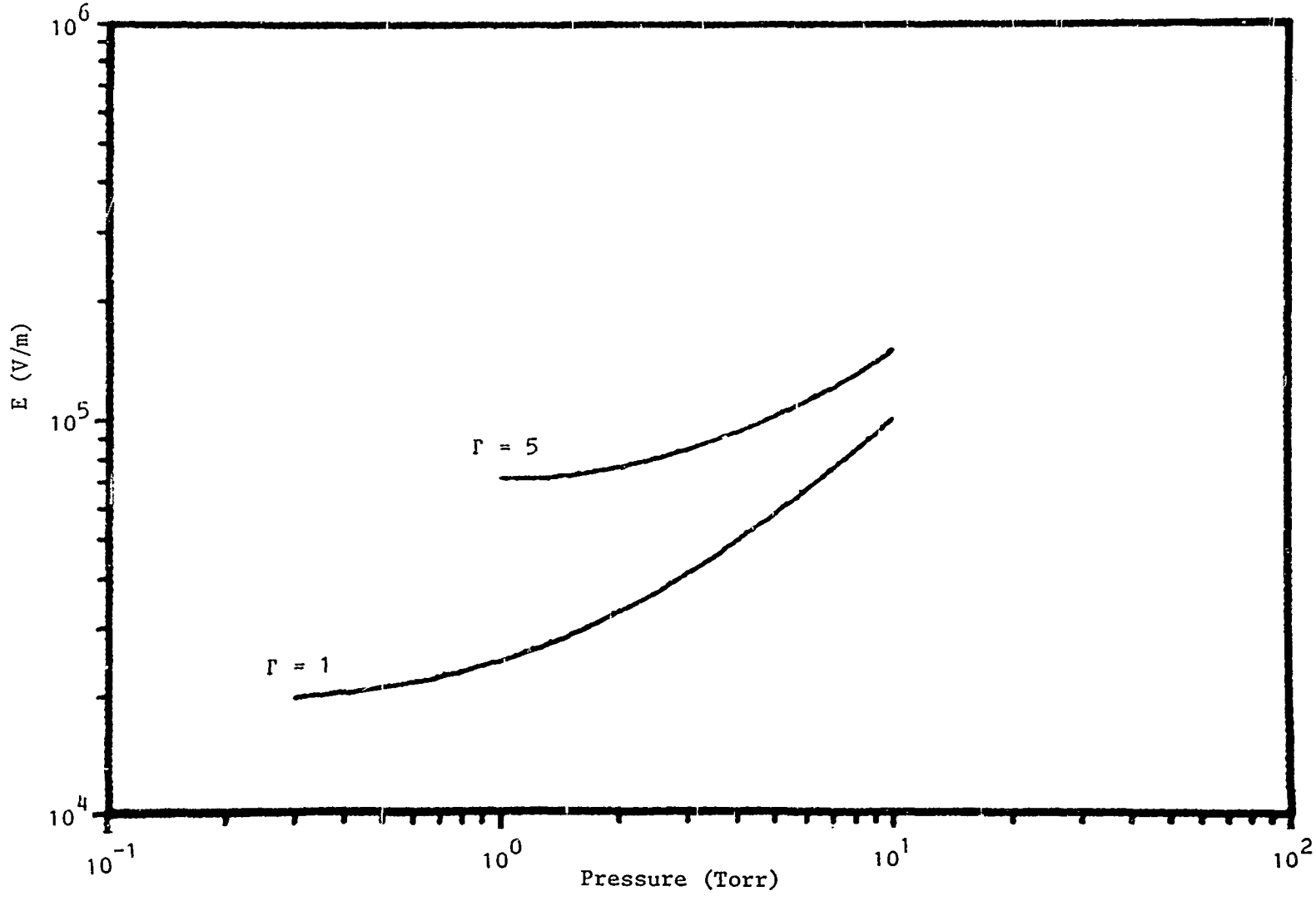

Figure 7g. (t(p) = 10E-8) sec.

Plots derived from Figure 6 to show contours for the e-fold levels $\Gamma = 1$ and $\Gamma = 5$ in the E-p plane for various pulse widths t_p:

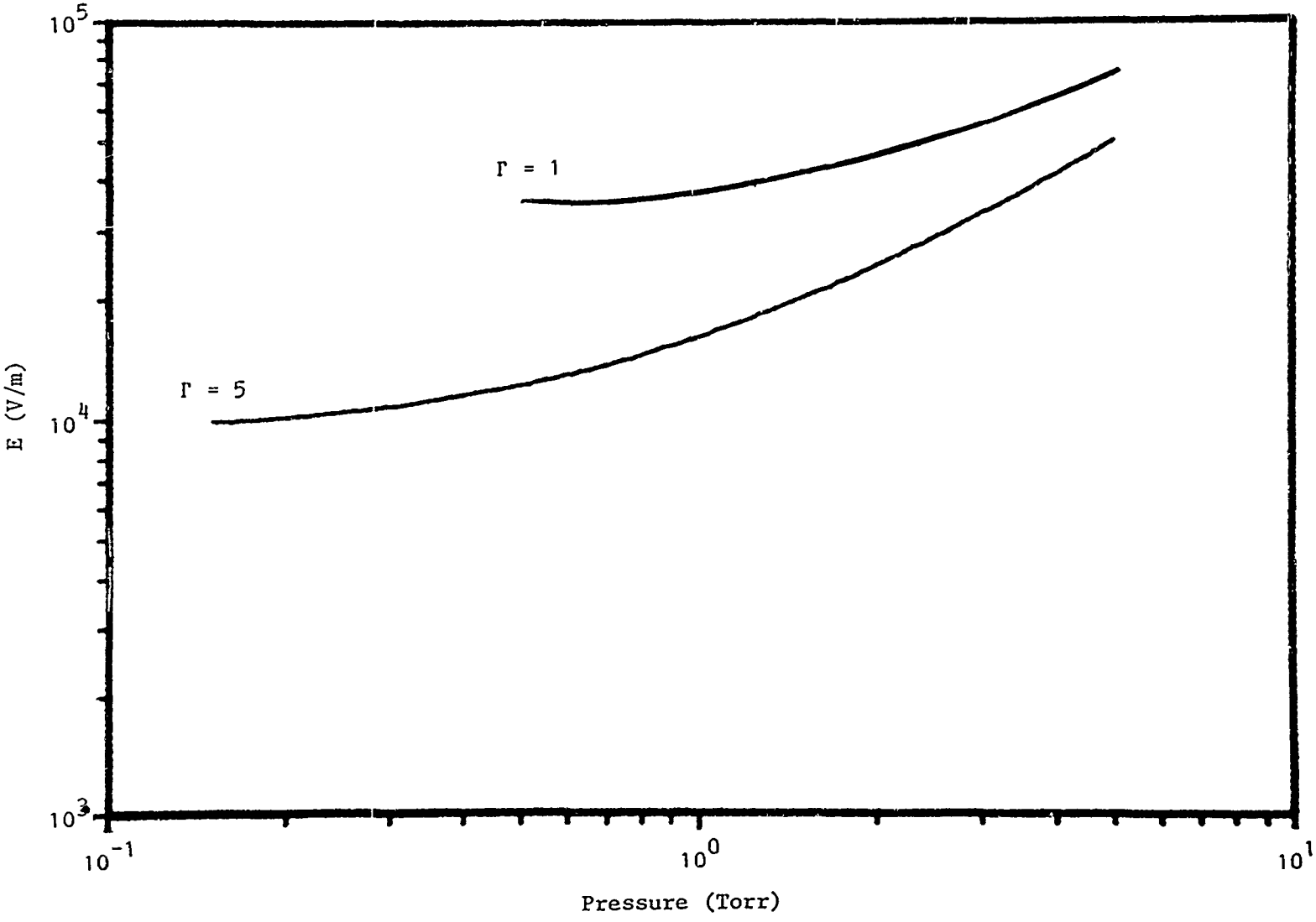

Figure 7h. (t(p) = 2x10E-8) sec.

Plots derived from Figure 6 to show contours for the e-fold levels $\Gamma = 1$ and $\Gamma = 5$ in the E-p plane for various pulse widths t_p:

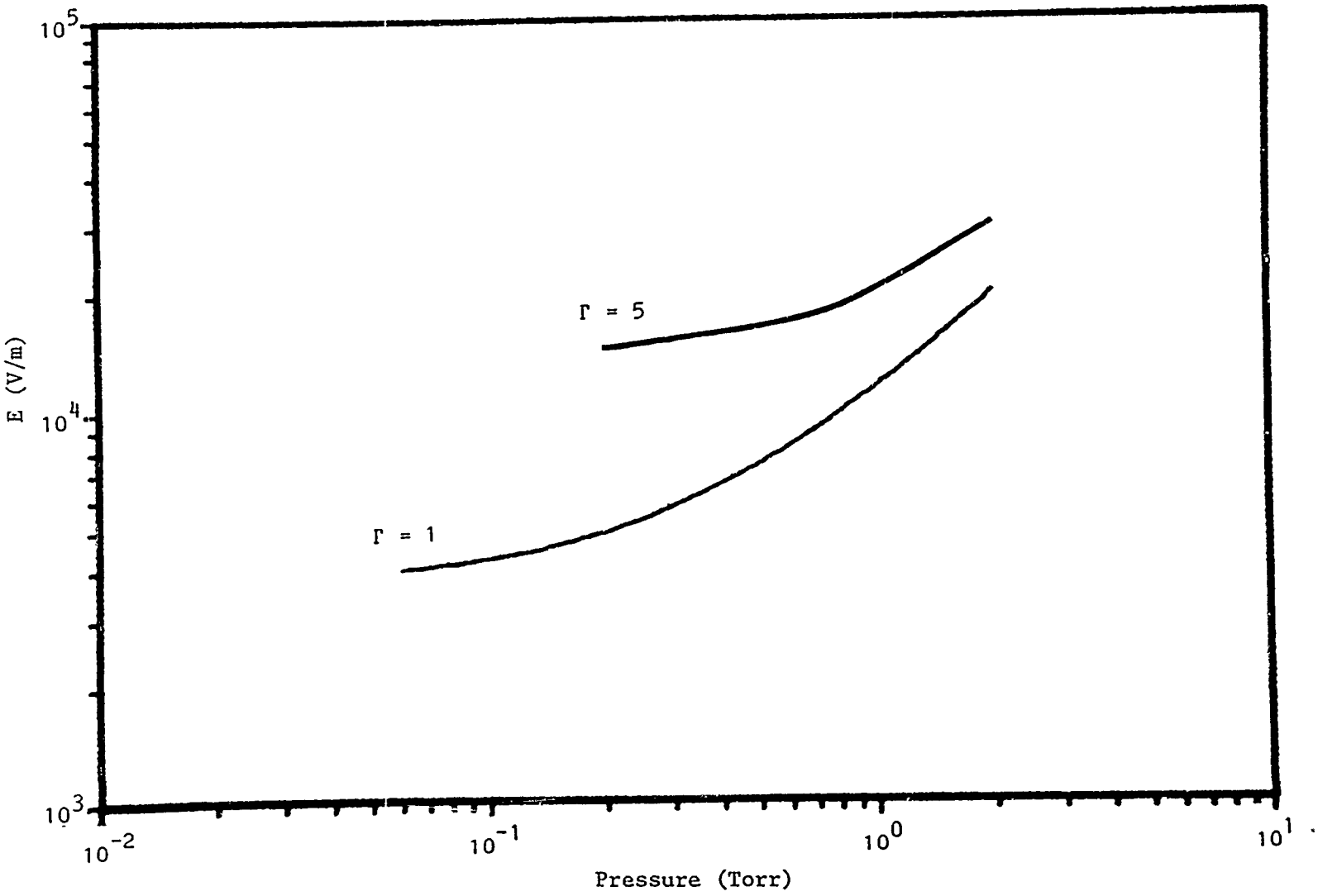

Figure 7i. (t(p) = 5x10E-8) sec.

Plots derived from Figure 6 to show contours for the e-fold levels $\Gamma = 1$ and $\Gamma = 5$ in the E-p plane for various pulse widths t_p:

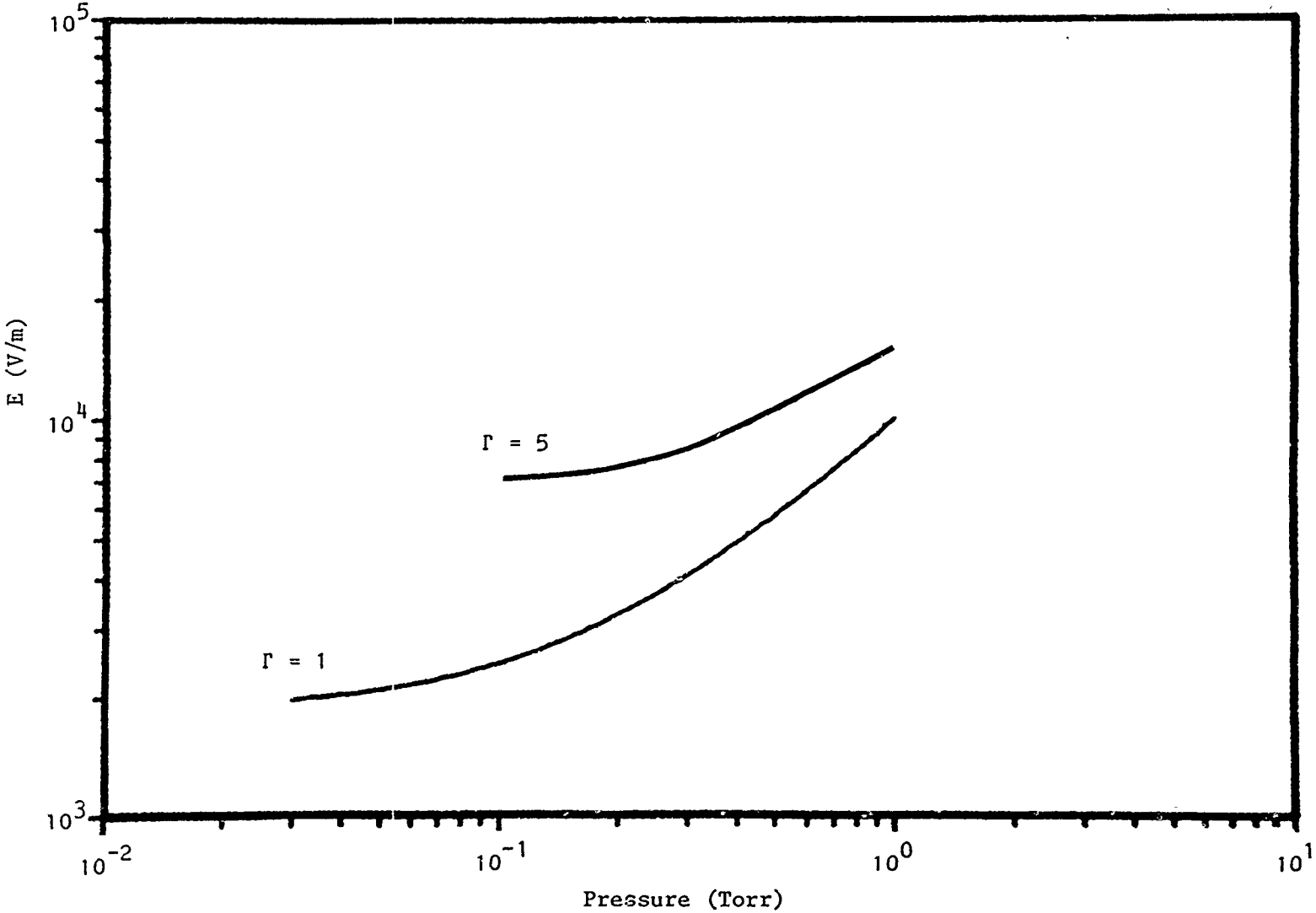

Figure 7j. (t(p) = 10E-7) sec.

APPENDIX A

The scaling relations associated with the transient expression for the collisonal ionization frequency caused by secondary electrons can be derived through general arguments. The equation for the electron distribution function for a uniform system with a constant electric field E can be written symbolically as

$$\frac{dF}{dt} = E \cdot G - N \cdot H \qquad (A\text{-}1)$$

where N is the neutral number density and G and H depend on the electron velocities and not explicitly on time. While Equation (A-1) generally represents a Boltzmann equation, it can also represent the simple electron equation of motion often used in heuristic descriptions of many particle systems. In this case

$$F \rightarrow v$$
$$G \rightarrow e/m$$
$$H \rightarrow \nu' v$$

where v is the particle velocity, e/m the charge to mass ratio for an electron, and ν' the secondary electron collision frequency per single neutral particle in a unit volume; the conventional drag frequency $\nu_m = \nu' N$.

It is simple to put Equation (A-1) in the form

$$\frac{dF}{d\xi} = \frac{E \cdot G}{N} - H \qquad (A\text{-}2)$$

where $\xi = Nt$. It is immediately seen from Equation (A-2) that for a given E/N (or equivalently E/p, where p is pressure) the time evolution for F varies inversely with N (or p). In steady state F becomes independent of ξ and depends on E/p alone.

The transient collisional ionization frequency has been calculated by Bloomberg and Pine (1984). Time variation of the collision frequency can be approximated by the expression

$$\nu = \bar{\nu} \left(1 - e^{-t/td}\right) \tag{A-3}$$

where t_d is a delay time obtained from the numerical results of the Monte Carlo algorithm; $\bar{\nu}$ is the steady state collisional ionization frequency. From the scaling results discussed above we can write

$$t_d = f(E/p)/p \tag{A-4}$$

$$\bar{\nu} = p\, g(E/p) \tag{A-5}$$

The collisonal ionization e-folding over a time interval, t_p, is

$$\Gamma = \int_0^{t_p} \nu dt \tag{A-6}$$

Substitution of Equation (A-3) into Equation (A-6) and use of Equations (A-4) and (A-5) gives

$$\Gamma = g\left[pt_p + f \exp\{-pt_p/f\} - f\right] \tag{A-7}$$

which expression was reproduced in the main Text as Equation (5a).

The increase in the number of electrons created in the avalanche of a single secondary electron over a time interval t_p is just $\exp(\Gamma)$. Use of the steady state value for the collisional ionization over the entire time interval t_p overestimates the avalanche by the factor

$$\exp\{gpt_p - \Gamma\} = \exp\{fg\left[1 - \exp(-pt_p/f)\right]\} \tag{A-8}$$

APPENDIX B

THERMALIZATION OF SECONDARY ELECTRONS UNDER AMSGEMP CONDITIONS

Howard W. Bloomberg
Vernon W. Pine

Beers Associates, Inc.
P.O. Box 2549, Reston, VA 22090

Abstract

A Monte Carlo algorithm is used to determine the time behavior of source secondary electrons for ranges of the electric field to pressure ratio E/p of interest in AMSGEMP. The algorithm contains a very detailed cross section set describing electron interactions with the background gas. We show that the delay in the attainment of the peak time independent ionization frequency (or ionization coefficient) may result in negligible ionization over times of interest. In any case the behavior is shown to behave much differently than in examples where limited cross section sets, common in currently employed predictive codes, are employed. In particular, the importance of momentum transfer is indicated. A critique of the scaling implications of the phenomena is made.

1. Introduction

The study of air modified SGEMP-AMSGEMP requires the understanding of secondary electron behavior over a wide range of electric fields and ambient pressure[1-4]. The maximum electric field, associated with the Child-Langmuir space charge limit for photoemitted electrons, is about 5×10^6 V/m, whereas the pressure range for which X-ray penetration is important is vacuum to about 10 Torr. These numbers imply a wide range for the electric field to pressure ratio E/p, the traditional parameter against which electron swarm transport quantities are specified. A last general parameter of interest in AMSGEMP problem is the radiation pulse width, which ranges through tens of nanoseconds.

While the behavior of secondary electrons is essential to AMSGEMP, the models developed thus far are not adequate to describe these electrons for the wide range of parameters of interest. Indeed, the models describe accurately only two extremes in parameter space. The first is for low E/p, where the secondaries approach a steady state distribution within times much shorter than the radiation pulse width. In this case the swarm theory[5] description is applicable. The second extreme is for high E/p where each secondary reaches a very large energy and all interactions except for collisional ionization can be neglected. In this case no distinction is made between secondary and high energy primary photoemitted electrons.

In this work we determine the transient properties of the secondary electron population caused by initiatory electrons moving within given constant electric fields and interacting with N_2 at arbitrary pressures. The problem is addressed through a Monte Carlo approach. Monte Carlo techniques have been used extensively to study the transient effects of electron swarms in the pre-breakdown phase of gas discharges[6-9]. Besides applying Monte Carlo to parameters of interest in AMSGEMP, we have generalized previous work in several ways. First, we have incorporated into the algorithm accurate cross section sets for energy loss due to excitation as well as collisional ionization. In addition, we include the effects of elastic scattering through use of momentum transfer cross sections. We also have speeded up the previous calculations for determination of the mean free times for a particle history, when the particle energy changes appreciably between collisons. Finally, we have employed sampling techniques to enable us to find important history averaged information such as velocity drift and the ionization coefficient with the use of a relatively small number of histories. Thus, useful computations were carried out with nominal computer times even with the detailed cross section sets.

The algorithm is described in Section 2. In Section 3 it is shown how the secondary temperatures, drift velocity evolve to steady state as a function of electric field and pressure. We benchmark the steady state values for the ionization coefficients against the tabulated results of Dutton[5] for various E/p. We show how the approach to steady state depends on the electric field even though steady state values depend only on E/p. In Section 4 the results of the Monte Carlo algorithm are shown when a limited cross section set, characteristic of the interactions employed in current AMSGEMP computer simulations, is used in place of the complete set. Results for the two cross sections are compared. In Section 5 results are discussed. We define the limits of applicability of AMSGEMP algorithms as a function of the X-ray pulse width. We indicate the importance of the errors resulting from the limited cross section set.

2. Single Scatter Monte Carlo

The algorithm described here was incorporated into an existing code SEMC[10] (Single Electron Monte Carlo) developed to solve for electron properties in the limit of large enough times such that transport coefficients can be defined. Here we discuss those changes needed to compute time dependent properties of secondary electrons in N_2. Many features of SEMC were retained in the modification for explicitly transient behavior. Among these were the scorings to determine the velocity distribution functions, as well as the scattering kernel formulation. The last procedure connects the Monte Carlo approach to the Boltzmann equation. In a practical sense, it also is given a convenient format for the input specification of detailed tabulated cross section sets for arbitrary background materials.

Algorithm for Transient Effects.

The problem is to determine secondary electron properties evolving from a set of initiatory electrons existing within an N_2 background in the presence of a constant electric field. In the spirit of the single scatter Monte Carlo approach we can imagine a single electron being launched at time zero.

The electron undergoes collisions with the background during the course of its history ending after a specified time interval. For a sufficiently large energy the electron creates an ion pair through collisional ionization. This second particle created some time after time zero, should also be tracked by the algorithm. Since all histories end at the same time, the lifetime of the second electron is shorter than the first. More particles are created as the avalanche proceeds. Within the time interval of interest a finite number of electrons will be created, and, in principle, all of them could be tracked. To improve statistics a second electron could be launched at time zero, and the entire process could be repeated. The difficulty with this straightforward selection of electron histories is that the total number of histories cannot be chosen prior to the calculation. The cost of such a run cannot be controlled a priori. To control this problem we specify initially the number of time histories to be tracked in a code run. The first particle history is launched at time zero. We count the number of ionizations created by the particles and thereby obtain a first estimate to the ionization rate, time averaged over the time interval of interest. The second particle history commences at either time zero or at one of the times when an ionization event took place. The choice for the launch time of the second particle is determined by a Monte Carlo selection from the distribution of particles over the complete time interval determined by avalanche statistics. This means that electrons created by collisional ionization late in time have a higher probability of being selected for a launch. The procedure is then repeated. The initial times for candidate particle histories are time zero and those times for which ionizations occurred in all previous histories. The distribution used to determine the time for each launch is determined from statistical information obtained in all previous histories. For simplicity, this analysis considers that, at the beginning of each time history, the electron is at rest.

For sufficiently high E/p a number of particles may run away over the time interval of interest. Runaways are a component of the secondary electron population that are difficult to incorporate into simple swarm theory. In large constant electric fields they continually take energy from the field. In a realistic situation the energy that the electric field can give to an electron must be limited, but the assignment of a limit necessarily brings into play the parameter of a particular configuration. In AMSGEMP problems we have selected 10 keV as the limiting secondary electron energy. This corresponds to about the largest potential difference that can be sustained by the primary photoemitted electrons. For our purposes the transient swarm properties are not sensitive to the prescribed runaway cut off energy, since multi keV electrons contribute negligibly to the ionization coefficients when the bulk of the secondaries have energies less than 1 keV.

In Figure 1 we show a schematic diagram illustrating the types of time histories considered over a specified time interval t_s. Only those particles that end their histories at t_s contribute to the velocity distribution function, that is no velocity information from runaways is retained. On the other hand, the contribution to collisional ionization of all histories prior to possible runaway are included.

Collision Cross Sections.

Elastic and inelastic collision cross sections have been incorporated into the numerical algorithm to describe electron interaction with the background N_2. Besides ionization important excitation cross sections were included in the set of inelastic cross sections. These data were obtained from sources compiled by Strickland et al.[11].

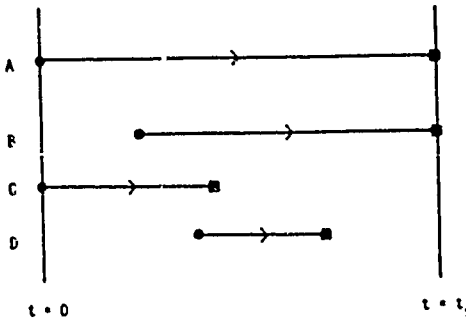

Figure 1. Four Types of Electron Histories

A. An initiatory electron launched at $t = 0$ and ending its history at the prescribed time $t = t_s$;

B. An electron created at $t > 0$ in the avalanche and ending its history at $t = t_s$;

C. An initiatory electron that runs away at $t < t_s$;

D. An avalanche created electron running away at $t < t_s$.

The momentum transfer coefficients were computed from differential elastic cross section sets from Shyn et al.[12] below 70 eV, and from Bromberg[13] below 500 eV. The momentum transfer cross section is related to the differential cross section by the formula

$$\sigma_m(U) = 2\pi \cdot \int \frac{d\sigma}{d\Omega} \sin\nu(1 - \cos\nu)\, d\nu \qquad (1)$$

In general a numerical computation of this equation must be carried out. For energies above 1 keV we use the form for the screened Rutherford potential used by Strickland et al.[12].

The cross sections were used to determine collisional events for each electron history. The particle collision frequency $\nu(U)$ is related to the sum of all cross sections $\sigma_i(U)$ for a particular energy U by the expression

$$\nu_T(U) = \sigma_T(U) \cdot \sqrt{2U/m} \qquad (2)$$

The time for a collision to occur is related to a random number ζ between 0 and 1 and the mean frequency by the formula

$$\ln(1 - \zeta) = -\int_0^t \nu_T(U)dt \qquad (3)$$

where ν_T is evaluated for the changing energy of the electron experiencing between collisions the constant acceleration from the electric field directed along the z-axis, E. Once the logarithm is determined by selection of the random number the integration is carried out in time until the prescribed value of the integral is reached. This procedure defines the time interval until the next collision. It is relatively easy to perform even when ν_T varies considerably over the integration range.

Once the time for the next collision has been established one needs to determine the type of collision. This is obtained by consideration of the relative weight of all cross sections. The specific collision type is found by random number selection. The effect of inelastic collisions is that the particle loses a specified energy with no directional change of velocity vector while particles undergo a change of direction based upon an isotropic distribution when they transfer momentum.

In Figure 2 we summarize the cross section information as a function of electron energy. The pressure normalized momentum transfer frequency ν_m/p is defined in terms of momentum transfer cross section σ_m by the relation

$$\nu_m/p = \sigma_m v\bar{N} \qquad (4)$$

where $\bar{N}$ is the number density of N_2 corresponding to a pressure of 1 torr: $\bar{N} = 3.55 \times 10^{16}$ cm^{-3}, v is the electron velocity. The second plot is the energy loss rate normalized to pressure. Here ν_u/p is related to the loss function L(E) by the relation

$$\nu_u/p = vL(U)/U \cdot \bar{N} \qquad (5)$$

where the loss function represents the energy loss from all important channels. In our case we consider several collisional excitation loss mechanisms as well as the collisional ionization energy loss channel. Therefore,

$$L(U) = \sum_i \sigma_e^{(i)} \varepsilon_i + \sigma_I \varepsilon_I \qquad (6)$$

where the sum extends over all important excitation channels; $\sigma_e^{(i)}$ is the cross section for the i^{th} type of excitation while ε_i is the energy lost through this channel. σ_I is the ionization cross section and ε_I is the energy lost in ionization, thus in N_2, ε_I = 15.6 eV.

3. Solutions

In Figure 3 we plot the cumulatively averaged ionization coefficient and the instantaneous drift velocity as functions of time. We have selected the steady state value of the ionization coefficient as the time dependent transport coefficient quoted in the electron swarm literature. We have compared the steady state ionization coefficients for various values of E/p with the results of a data survey conducted by Dutton[5]. The good agreement shown in Figure 4 gives credence to the accuracy of the detailed cross section set used in the analysis. The discrepancy at $E/p = 10^5$ V x m^{-1} x torr^{-1} is not unexpected. First it occurs at a high enough value of E/p where runaways might occur so that the data will be less reliable. Secondly, the loss function employed in the analysis neglects the kinetic energy imparted to the electrons created by collisional ionization. This source of energy loss for ionizing electrons becomes important for high electron energies.

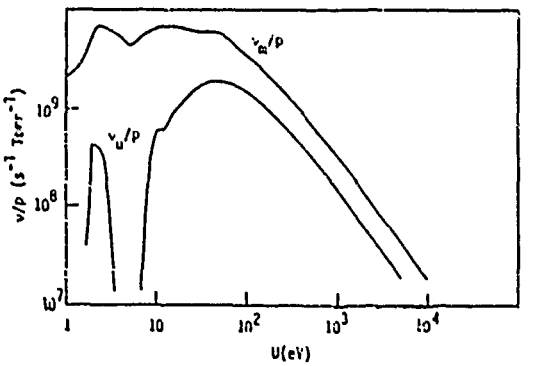

Figure 2. Momentum Transfer Rate and Energy Loss Rate in N_2 Normalized to Pressure as Functions of Electron Energy

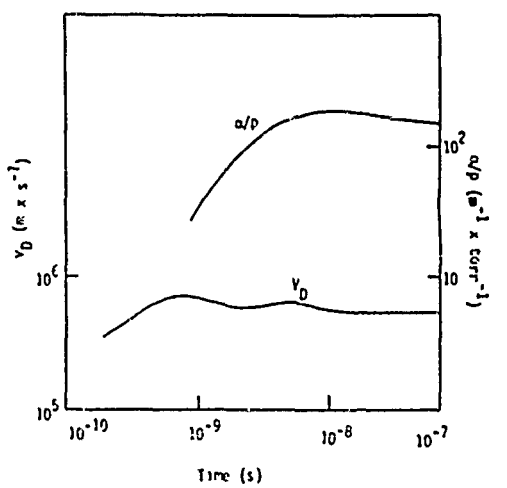

Figure 3. Drift Velocity and Cumulatively Averaged Ionization Coefficient as Functions of Time. Parameters are $E_z = 2 \times 10^4$V x m^{-1}, p = 1 torr. 500 histories were launched.

Although the asymptotic transport coefficients for electron swarms depend only on the parameter E/p, the rate at which these coefficients reach the asymptotic value depends on the value of the field. In fact, consideration of the Boltzmann equation equivalent to the Monte Carlo procedure shows that there exists a simple scaling for the rise times. Assume that the rise time for some property computed for a given E and p is t_r. Then for the case where

another field value E' = kE and another pressure p' = kp, where k is any constant, the corresponding rise time is related to the computed time by the relation $t_r = t_r/k$. The Monte Carlo algorithm produces the required scaling. This is shown in Figure 5 where the pressure normalized ionization frequency is plotted against time for $E = 2 \times 10^3$ V x m^{-1} and $E = 2 \times 10^4$ V x m^{-1} when $p = 10^{-1}$ torr and 1 torr, respectively.

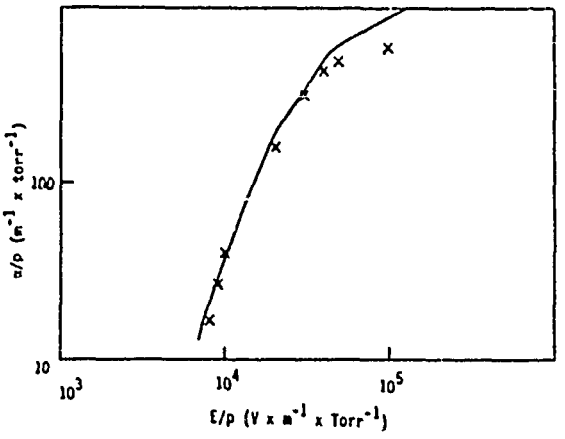

Figure 4. Steady State Ionization Coefficient vs E/p (from Dutton). The values obtained in this work are shown by the X's.

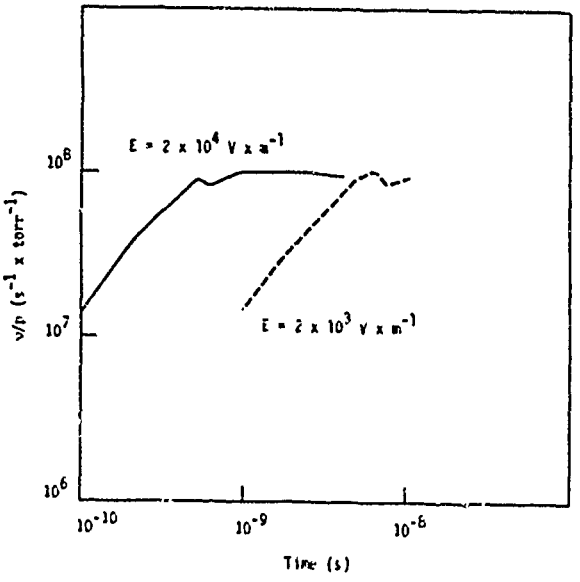

Figure 5. Cumulative Ionization Rate vs. Time for E = 2 x 10^3 and E = 2 x 10^4 V x m^{-1}. In each case E/p = 2 x 10^4 x m^{-1} x torr 1.

4. Comparison with Limited Cross Section Set

The particle pushing algorithms used for experimental predictions in the AMSGEMP community generally exclude the effects of elastic scattering and energy loss through discrete excitation. Generally, the only electron background interaction included is that for collisional ionization. To test the effect of excluding the elastic and excitation interactions we have limited the original cross section set to include only the collisional ionization cross section. The results of those runs were compared to runs with the same parameters when the complete cross section set was employed.

The results are plotted in Figures 6 and 7. In Figure 6 we show the drift velocities as functions of time. It is apparent that the limited cross section set gives rise to drift velocities that reach steady state values about 6 times higher than the corresponding drift velocities obtained with the complete cross section. The values of the drift velocity for the latter case agrees well with the data reported by Dutton[5]. A large discrepancy is also shown in Figure 6 where the cumulatively averaged ionization coefficient is plotted against time. The ionization coefficient for the limited set peaks early at a much higher value than for the case of the complete set. The steady state values achieved for this case again agrees well with the data of Dutton (see Figure 4).

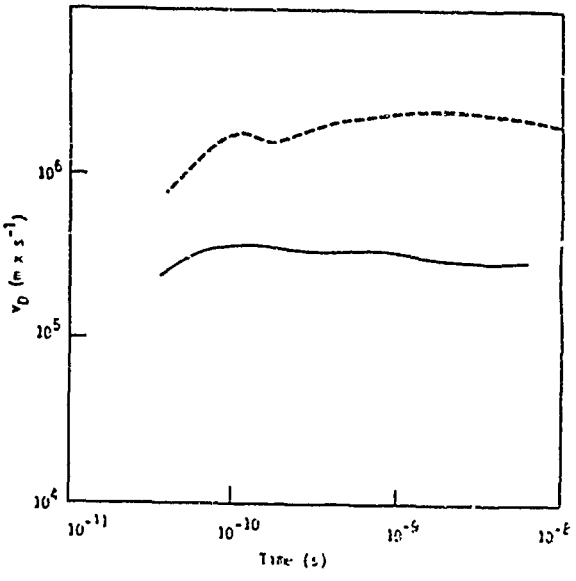

Figure 6. Drift Velocity Versus Time

The solid curve is the numerical result for the complete interaction cross section set, while the dashed curve is the result for the limited cross section set. Parameters are $E = 10^5$ V x m^{-1}, p = 10

5. Discussion of Results

We have shown large discrepancies in ionization coefficients (and ionization rates) between the results with a complete cross section and with a limited set approximating the treatment of secondaries in present AMSGEMP predictions codes. The

discrepancies are most severe at low E/p where the momentum transfer rates and excitation processes are very important. At higher E/p, where the secondaries have larger energies, excitation processes and momentum transfer rates no longer strongly dominate the collision ionization processes. Thus, the discrepancies in the results, while significant, are not as severe.

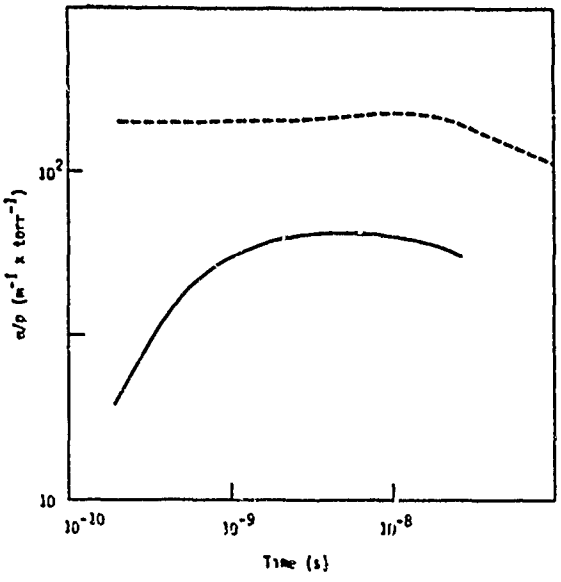

Figure 7. Cumulatively Averaged Ionization Coefficient Versus Time.

The solid curve is the numerical result for the complete interaction cross section, while the dashed curve is the result for the limited cross section set. Parameters are E = 10^5 V x m^{-1}, p = 10 torr.

The fundamental question to be asked in AMSGEMP phenomena is whether the discrepancies affect the physics. The key parameter is the ratio of the ionization rate with the characteristic frequency of the radiation pulse. If this ratio is small, than the avalanche may not be an important effect, since the initiatory electrons are being generated at a rate of order the inverse of the characteristic radiation pulse width. Since the avalanche ionization rate is small for low E/p, the large discrepancies observed when one uses a complete cross set compared to the limited set may not affect the physics. This is particularly true for a given E/p when p is small. Then the transient rise time of the ionization rate to its asympotic value may be even larger than the radiation pulse width, and the effect of secondary avalanche could be neglected altogether.

At larger E/p when the ionization rate becomes larger, the discrepancies in the use of the complete cross section set as compared to the limited set are still significant. Generally, particles that are not programmed to undergo momentum transfer interactions rapidly accelerate to velocities where the ionization rate is very high. However, the particles may run away at later times and then contribute little to ionization. Results from the complete and limited cross section sets show this effect in Figure 8, where it is seen that the ionization rates are large enough that they generally would be important in X-ray pulse experiments. This confirms our recommendation that momentum transfer should be included in models for secondary electrons, even for those at high energies.

The results, while desired for N_2, should be applicable to air as well. The de-excitation cross sections for O_2 partially fill in the depression in the energy loss rate curve in Figure 2 between the electron energies 5 and 10 eV. The change should not influence the qualitative nature of the results presented here. Attachment of secondary electrons to the electronegative O_2 molecule is an effect that has been neglected. For the large field strengths of interest in AMSGEMP it would not appear that this effect would have important consequences on the results presented here. There is no intrinsic difficulty in incorporating either effect into the existing algorithm.

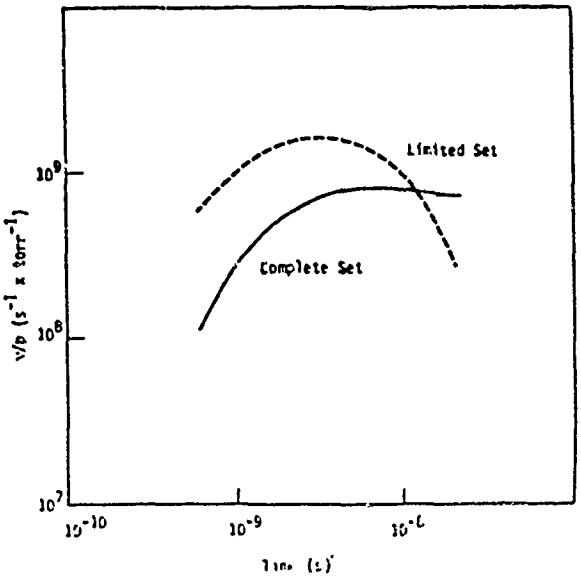

Figure 8. Cumulative Ionization Rates versus Time for the Complete and limited Cross Section Sets. Parameters are E = 5 x 10^4 V x m^{-1} and p = 1 torr. 500 histories were followed in each computer run.

6. References

1. T. A. Tumolillo, J. P. Wondra, J. Bombardt, G. Merkel, and D. Spohn, Pres.-3D: "A Computer Code for the Self-Consistent Solution of the Maxwell-Lorentz Three-Species Air Chemistry Equations in Three Dimensions", IEEE Trans. Nucl. Sci., NS-24(6), 2456-2460, Dec. 1977.

2. B. M. Goldstein and R. Stettner, "Fluid Treatment of Runaway Electrons in Strong Electric Fields", IEEE Trans. Nuc. Sci., NS-26(6), 5006-5011, Dec. 1979.

3. A. J. Woods, W. E. Hobbs. E. P. Wenaas, "Air Effects on the External SGEMP Response of a Cylinder", IEEE Trans. Nucl. Sci., NS-28 (6), 4467-4472, Dec. 1981.

4. A. J. Woods, M. J. Treadaway. S. Nunan, and D. Higgins, "Air-Enhanced SGEMP Response - An Experimental and Analytical Investigation", IEEE Trans. Nuc. Sci., NS-29 (6), 1793-1797, Dec.1982.

5. J. Dutton, "A Survey of Electron Swarm Data," J. Phys. and Chem. Ref. Data, 4, 577, 1975.

6. A.I. McIntosh, "Computer Simulation of an Electron Swarm at Low E/p in Helium," Aust. J. Phys., 27(1), 59-71, Feb. 1974.

7. G.L. Braglia, "The Diffusion and Drift of Electrons in Gases: a Monte Carlo Simulation,", Physica B&C, 92 B&C(1) 91-112, Aug.-Sept., 1977.

8. I.D. Reid and S.R. Hunter, "Comparison between the Boltzmann and Monte Carlo Simulation Methods for the Determination of Electron Swarm Transport Coefficients in Molecular Hydrogen, Aust. J. Phys., 32 (3), 231-254, June 1979.

9. Y. Sakai, H. Tagashira, and S. Sakomoto, "The Development of Electron Avalanches in Argon at High E/N Values I. Monte Carlo Simulation", J. Phys. D,10(7), 1035-1049, May, 1977.

10. B.L. Beers, V.W. Pine, H.C. Hwang and H.W. Bloomberg, "Negative Streamer Development in FEP Teflon," IEEE Trans. Nuc. Sci., NS-26, 5127, 1979.

11. D.J. Strickland, D.L. Book, T.P. Coffey, and J.A. Fedder, "Transport Equation Techniques for the Deposition of Auroral Electrons," J. Geophys. Res. 81, 2755, 1976.

12. T.W. Shyn, R.S. Stolarski, and G.R. Carignan, "Angular Distribution of Electrons Elastically Scattered from N_2, Phys. Rev. A, 6(3), 1002-1012, Sept., 1972.

13. J.P. Bromberg, "Absolute Differential Cross Sections of Elastically Scattered Electrons," J. Chem. Phys., 52(4), 1713-1715, Feb., 1970.

DISTRIBUTION LIST

DEPARTMENT OF DEFENSE

ASSIST TO THE SECY OF DEF ATOMIC ENERGY
ATTN: EXECUTIVE ASSISTANT

COMMANDER IN CHIEF, ATLANTIC
ATTN: J36

DEFENSE ADVANCED RSCH PROJ AGENCY
ATTN: J FRASER
ATTN: R REYNOLDS
ATTN: S ROOSILD

DEFENSE COMMUNICATIONS ENGINEER CENTER
ATTN: CODE R410
ATTN: CODE R720 C STANSBERRY

DEFENSE ELECTRONIC SUPPLY CENTER
ATTN: DEFC-EAA

DEFENSE INTELLIGENCE AGENCY
ATTN: DB-6E
ATTN: DT-1B
ATTN: RTS-2B

DEFENSE LOGISTICS AGENCY
ATTN: DLA-QEL K MASON
ATTN: DLA-SEE F HARRIS

DEFENSE NUCLEAR AGENCY
3 CYS ATTN: RAEV TREE
4 CYS ATTN: STTI-CA

DEFENSE TECHNICAL INFORMATION CENTER
12 CYS ATTN: DD

FIELD COMMAND DNA DET 2
LAWRENCE LIVERMORE NATIONAL LAB
ATTN: FC-1

DNA PACOM LIAISON OFFICE
ATTN: J BARTLETT

FIELD COMMAND DEFENSE NUCLEAR AGENCY
ATTN: FCPF R BLACKBURN
ATTN: FCPR
ATTN: FCTT
ATTN: FCTT W SUMMA
ATTN: FCTXE

JOINT CHIEFS OF STAFF
ATTN: C3S EVAL OFFICE HDOO

JOINT DATA SYSTEM SUPPORT CTR
ATTN: C-312 R MASON
ATTN: C-330

JOINT STRAT TGT PLANNING STAFF
ATTN: JLK ATTN: DNA REP
ATTN: JLKS
ATTN: JPPFD
ATTN: JPTM

NATIONAL COMMUNICATIONS SYSTEM
ATTN: NCS-TS
ATTN: NCS-TS D BODSON

UNDER SECY OF DEF FOR RSCH & ENGRG
ATTN: STRAT & SPACE SYS (OS)
ATTN: STRAT & THEATER NUC FOR F VAJDA

DEPARTMENT OF THE ARMY

BDM ADVANCED TECHNOLOGY CENTER
ATTN: ATC-O F HOKE
ATTN: ATC-T

FORT HUACHUCA
ATTN: TECH REF DIV

HARRY DIAMOND LABORATORIES
ATTN: C FAZI
ATTN: DELHD-NW-EA J MILETTA
ATTN: DELHD-NW-P T FLORY
ATTN: DELHD-NW-R F MCLEAN 22300
2 CYS ATTN: DELHD-NW-RA W VAULT
ATTN: DELHD-NW-RH
ATTN: SCHLD-NW-P
ATTN: SLCHD-NW-EC
ATTN: SLCHD-NW-R
ATTN: SLCHD-NW-RA
ATTN: SLCHD-NW-RC
ATTN: T TAYLOR

NUCLEAR EFFECTS DIVISION
ATTN: R WILLIAMS

U S ARMY ARMOR & ENGINEER BOARD
ATTN: ATZK-AE-AR J DENNIS

U S ARMY BALLISTIC RESEARCH LAB
ATTN: SLCBR-VL D RIGOTTI

U S ARMY BELVOIR RD & E CTR
ATTN: DRDME-E J BOND JR

U S ARMY COMMUNICATIONS R&D COMMAND
ATTN: DRSEL-NL-RO R BROWN

U S ARMY ELECTRONIC TECH DEV LAB
ATTN: SLCET-SI R ZETO

U S ARMY ENGINEER DIV HUNTSVILLE
ATTN: HNDED-ED J HARPER

U S ARMY MATERIAL TECHNOLOGY LABORATORY
ATTN: DRXMR-B J HOFMANN
ATTN: DRXMR-HH J DIGNAM

U S ARMY NUCLEAR & CHEMICAL AGENCY
ATTN: LIBRARY

U S ARMY RESEARCH OFFICE
ATTN: R GRIFFITH

DEPARTMENT OF THE ARMY (CONTINUED)

U S ARMY STRATEGIC DEFENSE CMD
ATTN: BMDSC-AV J HARPER
ATTN: BMDSC-HW R DEKALB
ATTN: BMDSC-LEH R C WEBB
ATTN: DASD-H-SAV

U S ARMY STRATEGIC DEFENSE COMMAND
ATTN: DASD-H-SA R C WEBB
ATTN: DASD-H-YD F HOKE

U S ARMY TEST AND EVALUATION COMD
ATTN: AMSTE-

U S ARMY TRADOC SYS ANALYSIS ACTVY
ATTN: ATAA-TFC O MILLER

U S ARMY WHITE SANDS MISSILE RANGE
ATTN: STEWS-TE-AN A DE LA PAZ
ATTN: STEWS-TE-AN J MEASON
ATTN: STEWS-TE-AN R DUTCHOVER
ATTN: STEWS-TE-AN R HAYS
ATTN: STEWS-TE-N K CUMMINGS
ATTN: STEWS-TE-N T ARELLANES
ATTN: STEWS-TE-NT M SQUIRES

USA MISSILE COMMAND
ATTN: AMSMI-LC-FS, G. THURLOW
3 CYS ATTN: DOCUMENTS SECTION BLDG 4484
ATTN: DRCPM-PE-EA W WAGNER
ATTN: HAWK PROJ OFCR DRCPM-HAER

XM-1 TANK SYSTEM
ATTN: DRCPM-GCM-SW

DEPARTMENT OF THE NAVY

LEAHY CG 16
ATTN: WEAPONS OFFICER

NAVAL AIR SYSTEMS COMMAND
ATTN: AIR 310
ATTN: AIR 350F
ATTN: AIR 54053

NAVAL AVIONICS CENTER
ATTN: CODE B415 D REPASS

NAVAL INTELLIGENCE SUPPORT CTR
ATTN: NISC LIBRARY

NAVAL OCEAN SYSTEMS CENTER
ATTN: CODE 9642B TECH LIB

NAVAL POSTGRADUATE SCHOOL
ATTN: CODE 1424 LIBRARY

NAVAL RESEARCH LABORATORY
ATTN: CODE 4040 J BORIS
ATTN: CODE 4154 J H ADAMS
ATTN: CODE 4600 D NAGEL
ATTN: CODE 4610 J RITTER
ATTN: CODE 4611 E PETERSON
ATTN: CODE 4612 D WALKER
ATTN: CODE 4612 R STATLER
ATTN: CODE 4613 A B CAMPBELL
ATTN: CODE 4614 L AUGUST
ATTN: CODE 4614 P SHAPIRO
ATTN: CODE 4652 G MUELLER
ATTN: CODE 4653 A NAMENSON
ATTN: CODE 4673 A KNUDSON
ATTN: CODE 4682 C DOZIER
ATTN: CODE 4682 D BROWN
ATTN: CODE 5813 N SAKS
ATTN: CODE 5313 W JENKINS
ATTN: CODE 5814 D MCCARTHY
ATTN: CODE 5814 M PECKERAR
ATTN: CODE 5816 E D RICHMOND
ATTN: CODE 5816 R HEVEY
ATTN: CODE 5816 R LAMBERT
ATTN: CODE 6810 J KILLIANY
ATTN: CODE 6816 H HUGHES

NAVAL SEA SYSTEMS COMMAND
ATTN: CODE 08K NEWHOUSE

NAVAL SURFACE WEAPONS CENTER
ATTN: CODE F31
ATTN: CODE F31 F WARNOCK
ATTN: CODE F31 K CAUDLE
ATTN: CODE H-20
ATTN: CODE H23 R SMITH
ATTN: F31 J DOWNS

NAVAL WEAPONS CENTER
ATTN: CODE 343 FKA6A2 TECH SVCS

NAVAL WEAPONS EVALUATION FACILITY
ATTN: CLASSIFIED LIBRARY

NAVAL WEAPONS SUPPORT CENTER
ATTN: CODE 3073 T ELLIS
ATTN: CODE 605 J RAMSEY
ATTN: CODE 6054 D PLATTETER

NUCLEAR WEAPONS TNG GROUP, PACIFIC
ATTN: CODE 32

OFC OF THE DEP ASST SEC OF THE NAVY
ATTN: L J ABELLA

OFC OF THE DEPUTY CHIEF OF NAVAL OPS
ATTN: NOP 985F

OFFICE OF NAVAL RESEARCH
ATTN: CODE 220 D LEWIS
ATTN: CODE 414 L COOPER
ATTN: CODE 427

SPACE & NAVAL WARFARE SYSTEMS CMD
ATTN: CODE 5045.11 C SUMAN
ATTN: CODE 50451
ATTN: NAVELEX 51024 C WATKINS
ATTN: PME 117-21

DEPARTMENT OF THE NAVY (CONTINUED)

STRATEGIC SYSTEMS PROGRAMS (PM-1)
ATTN: NSP-2301 M MESEROLE
ATTN: NSP-2430 J STILLWELL
ATTN: NSP-2701
ATTN: NSP-27331
ATTN: NSP-27334

DEPARTMENT OF THE AIR FORCE

AERONAUTICAL SYSTEMS DIVISION, AFSC
ATTN: ASD/ENACC R FISH
ATTN: ASD/ENESS P MARTH
ATTN: ASD/YH-EX J SUNKES

AIR FORCE CTR FOR STUDIES & ANALYSIS
2 CYS ATTN: AF/SAMI TECH INFO DIV

AIR FORCE GEOPHYSICS LABORATORY
ATTN: SULL

AIR FORCE INSTITUTE OF TECHNOLOGY
ATTN: AFIT/ENP C BRIDGMAN
ATTN: LIBRARY

AIR FORCE SYSTEMS COMMAND
ATTN: DLCAM
ATTN: DLW

AIR FORCE WEAPONS LABORATORY, AFSC
ATTN: NTAAB C BAUM
ATTN: NTC M SCHNEIDER
ATTN: NTCAS J FERRY
ATTN: NTCAS J MULLIS
ATTN: NTCOX R TALLON
ATTN: NTCT G GOSS
ATTN: NTCTR K HUNT
ATTN: NTCTR R MAIER
ATTN: SUL

AIR FORCE WRIGHT AERONAUTICAL LAB
ATTN: POE-2 J WISE
ATTN: POOC-1 N HARROLD

AIR FORCE WRIGHT AERONAUTICAL LAB
ATTN: AFWAL/AADE
ATTN: AFWAL/MLPO R HICKMOTT
ATTN: AFWAL/MLTE

AIR LOGISTICS COMMAND
ATTN: OO-ALC/MMEDD/HARD CONTROL
ATTN: OO-ALC/MMGR/DOC CONTROL

AIR UNIVERSITY LIBRARY
ATTN: AUL-LSE

BALLISTIC MISSILE OFFICE/DAA
ATTN: ENBE
ATTN: ENMG
ATTN: ENSN
ATTN: ENSN M WILLIAMS
ATTN: ENSN W WILSON
ATTN: SYST
ATTN: SYST L BRYANT

BALLISTIC MISSILE OFFICE/ABRES
ATTN: ENSN/H WARD

ELECTRONIC SYSTEMS DIVISION
ATTN: INDC

FOREIGN TECHNOLOGY DIVISION, AFSC
ATTN: TQTD B BALLARD

OFFICE OF SPACE SYSTEMS
ATTN: DIRECTOR

OKLAHOMA CITY AIR LOGISTICS CTR
ATTN: DMM/R WALLIS

ROME AIR DEVELOPMENT CENTER, AFSC
ATTN: RBR J BRAUER

ROME AIR DEVELOPMENT CENTER, AFSC
ATTN: ESR B BUCHANAN
ATTN: ESR J SCHOTT
ATTN: ESR W SHEDD

SPACE DIVISION
ATTN: ALT

SPACE DIVISION
ATTN: YAS

SPACE DIVISION
ATTN: YAR CAPT STAPANIAN

SPACE DIVISION
ATTN: YD

SPACE DIVISION
ATTN: YE

SPACE DIVISION
ATTN: YG

SPACE DIVISION
ATTN: YN

STRATEGIC AIR COMMAND
ATTN: INA

STRATEGIC AIR COMMAND
ATTN: NRI/STINFO

STRATEGIC AIR COMMAND
ATTN: XPFC

STRATEGIC AIR COMMAND
ATTN: XPFS

TACTICAL AIR COMMAND
ATTN: TAC/XPJ

3416TH TECHNICAL TRAINING SQUADRON ATC
ATTN: TTV

DEPARTMENT OF ENERGY

DEPT OF ENERGY ALBUQUERQUE OPNS OFC
ATTN: WSSB
ATTN: WSSB R SHAY

DEPARTMENT OF ENERGY (CONTINUED)

UNIVERSITY OF CALIFORNIA
LAWRENCE LIVERMORE NATIONAL LAB
ATTN: L-10 H KRUGER
ATTN: L-13 D MEEKER
ATTN: L-156 J YEE
ATTN: L-156 R KALIBJIAN
ATTN: L-53 TECH INFO DEPT LIB
ATTN: W ORVIS

LOS ALAMOS NATIONAL LABORATORY
ATTN: D LYNN
ATTN: MS K 551 E LEONARD

SANDIA NATIONAL LABORATORIES
ATTN: ORG 2100 B L GREGORY
ATTN: ORG 2110 W DAWES
ATTN: ORG 2115 J E GOVER
ATTN: ORG 2143 T DELLON
ATTN: ORG 2144 P V DRESSENDORFER
ATTN: ORG 2150 J A HOOD
ATTN: ORG 2320 J H RENKEN
ATTN: ORG 2321 L POSEY
ATTN: ORG 5143 J L DUNCAN
ATTN: T WROBEL

OTHER GOVERNMENT

CENTRAL INTELLIGENCE AGENCY
ATTN: OSWR/NED
ATTN: OSWR/STD/MTB

DEPARTMENT OF TRANSPORTATION
ATTN: ARD-350

NASA GODDARD SPACE FLIGHT CTR
ATTN: CODE 311.3 D CLEVELAND
ATTN: CODE 313 V DANCHENKO
ATTN: CODE 601 E STASSINOPOULOS
ATTN: CODE 660 J TRAINOR
ATTN: CODE 695 M ACUNA
ATTN: CODE 701 W N REDISCH
ATTN: CODE 724.1 M JHABVALA

NASA LEWIS RESEARCH CTR
ATTN: M BADDOUR

NASA HEADQUARTERS
ATTN: CODE DP B BERNSTEIN

NATIONAL BUREAU OF STANDARDS
ATTN: C WILSON
ATTN: CODE A305 K GALLOWAY
ATTN: CODE A327 H SCHAFFT
ATTN: CODE A347 J MAYO-WELLS
ATTN: CODE A353 S CHAPPELL
ATTN: CODE A361 J FRENCH
ATTN: CODE C216 J HUMPHREYS
ATTN: T RUSSELL

DEPARTMENT OF DEFENSE CONTRACTORS

ADVANCED RESEARCH & APPLICATIONS CORP
ATTN: L PALKUTI
ATTN: R ARMISTEAD

AEROJET ELECTRO-SYSTEMS CO
ATTN: D TOOMB
ATTN: P LATHROP

AEROSPACE CORP
ATTN: D FRESH
ATTN: D SCHMUNK
ATTN: G GILLEY
ATTN: I GARFUNKEL
ATTN: J REINHEIMER
ATTN: J STOLL
ATTN: J WIESNER
ATTN: J.B. BLAKE
ATTN: M DAUGHERTY
ATTN: P BUCHMAN
ATTN: R SLAUGHTER
ATTN: V JOSEPHSON
ATTN: W CRANE
ATTN: W KOLASINSKI

ALLIED CORP
ATTN: DOCUMENT CONTROL

ALLIED CORP
ATTN: E MEEDER

AMPEX CORP
ATTN: K WRIGHT
ATTN: P PEYROT

ANALYTIC SERVICES, INC (ANSER)
ATTN: A SHOSTAK
ATTN: J OSULLIVAN
ATTN: P SZYMANSKI

APPLIED SYSTEMS ENGRG DIRECTOR
ATTN: J P RETZLER NUC S V MANG

AVCO SYSTEMS DIVISION
ATTN: C DAVIS
ATTN: D SHRADER
ATTN: F350 D FANN
ATTN: W BRODING

BDM CORP
ATTN: C M STICKLEY

BDM CORP
ATTN: D WUNSCH

BEERS ASSOCIATES, INC
ATTN: B BEERS
2 CYS ATTN: H W BLOOMBERG

BOEING CO
ATTN: M/S 18-73 C ROSENBERG
ATTN: M/S 2R-00 A JOHNSTON
ATTN: M/S 2R-00 D EGELKROUT
ATTN: M/S 2R-00 E L SMITH
ATTN: M/S 2R-00 I ARIMURA
ATTN: M/S 2R-00 R CALDWELL
ATTN: M/S 20-51 M ANAYA
ATTN: M/S 8J-78 W DOHERTY
ATTN: M/S 83-66 H WICKLEIN
ATTN: M/S 88-43 O MULKEY
ATTN: M/S 9C-99 C DIXON

DEPT OF DEFENSE CONTRACTORS (CONTINUED)

BOOZ-ALLEN & HAMILTON, INC
ATTN: R CHRISNER

CALIFORNIA INSTITUTE OF TECHNOLOGY
ATTN: W PRICE, MS-83-122

CALSPAN CORP
ATTN: R THOMPSON

CHARLES STARK DRAPER LAB INC
ATTN: J BOYLE
ATTN: N TIBBETTS
ATTN: P GREIFF
ATTN: W D CALLENDER

CINCINNATI ELECTRONICS CORP
ATTN: L HAMMOND

CLARKSON COLLEGE OF TECHNOLOGY
ATTN: P J MCNULTY

COMPUTER SCIENCES CORP
ATTN: A SCHIFF

CONTROL DATA CORP
ATTN: D NEWBERRY

UNIVERSITY OF DENVER
ATTN: SEC OFCR FOR F VENDITTI

DEVELCO, INC
ATTN: G HOFFMAN

DIKEWOOD CORP
ATTN: TECH LIB FOR D PIRIO

E-SYSTEMS, INC
ATTN: K REIS

E-SYSTEMS, INC
ATTN: DIV LIB

EATON CORP
ATTN: A ANTHONY
ATTN: R BRYANT

ELECTRONIC INDUSTRIES ASSOCIATION
ATTN: J KINN

FMC CORP
ATTN: L STATES

FORD AEROSPACE & COMMUNICATIONS CORP
ATTN: H LINDER
ATTN: TECH INFO SVC

GARRETT CORP
ATTN: S ELLIOTT

GENERAL ELECTRIC CO
ATTN: D TASCA
ATTN: R BENEDICT
ATTN: R CASEY
ATTN: TECH LIB

GENERAL ELECTRIC CO
ATTN: G GATI MD-E184

GENERAL ELECTRIC CO
ATTN: B FLAHERTY
ATTN: G BENDER
ATTN: L HAUGE

GENERAL ELECTRIC CO
ATTN: C HEWISON
ATTN: D COLE

GENERAL ELECTRIC CO
ATTN: D PEPIN

GENERAL RESEARCH CORP
ATTN: A HUNT

GEORGE WASHINGTON UNIVERSITY
ATTN: A FRIEDMAN

GOODYEAR AEROSPACE CORP
ATTN: SEC CONT STATION

GRUMMAN AEROSPACE CORP
ATTN: J ROGERS

GTE GOVERNMENT SYSTEMS CORP
ATTN: J A WALDRON

HARRIS CORP
ATTN: E YOST
ATTN: W ABARE

HONEYWELL, INC
ATTN: D NIELSEN MN 14-3015
ATTN: R GUMM

HONEYWELL, INC
ATTN: J SCHAFER
ATTN: MS 725-5

HUGHES AIRCRAFT CO
ATTN: B CAMPBELL E1/E110

HUGHES AIRCRAFT CO
ATTN: R C HENDERSON

HUGHES AIRCRAFT CO
ATTN: W SCHENET

HUGHES AIRCRAFT CO
ATTN: MS-A2408 J HALL

HUGHES AIRCRAFT INTL SVC CO
ATTN: A NAREVSKY
ATTN: D SHUMAKE
ATTN: E KUBO
ATTN: W SCOTT

IBM CORP
ATTN: H MATHERS

IBM CORP
ATTN: J ZIEGLER

IBM CORP
ATTN: A EDENFELD
ATTN: N HADDAD

DEPT OF DEFENSE CONTRACTORS (CONTINUED)

IIT RESEARCH INSTITUTE
ATTN: I MINDEL

ILLINOIS COMPUTER RESEARCH, INC
ATTN: E S DAVIDSON

INSTITUTE FOR DEFENSE ANALYSES
ATTN: TECH INFO SERVICES

INTEL CORP
ATTN: T MAY

IRT CORP
ATTN: J AZAREWICZ
ATTN: J HARRITY
ATTN: M ROSE
ATTN: MDC
ATTN: N RUDIE
ATTN: R MERTZ

JAYCOR
ATTN: M TREADAWAY
ATTN: R STAHL
ATTN: T FLANAGAN

JAYCOR
ATTN: C ROGERS
ATTN: R POLL

JOHNS HOPKINS UNIVERSITY
ATTN: P PARTRIDGE
ATTN: R MAURER

JOHNS HOPKINS UNIVERSITY
ATTN: G MASSON DEPT OF ELEC ENGR

KAMAN SCIENCES CORP
ATTN: C BAKER
ATTN: DIR SCIENCE & TECH DIV
ATTN: J ERSKINE
ATTN: N BEAUCHAMP
ATTN: W RICH

KAMAN SCIENCES CORP
ATTN: E CONRAD

KAMAN TEMPO
ATTN: DASIAC
ATTN: R RUTHERFORD
ATTN: W MCNAMARA

KAMAN TEMPO
ATTN: DASIAC

LITTON SYSTEMS, INC
ATTN: E L ZIMMERMAN
ATTN: F MOTTER

LOCKHEED MISSILES & SPACE CO, INC
ATTN: C JUNGA 95-43
ATTN: J SMITH
ATTN: REPORTS LIBRARY

LOCKHEED MISSILES & SPACE CO, INC
ATTN: A BOROFSKY
ATTN: B KIMURA
ATTN: E HESSEE
ATTN: J C LEE
ATTN: J CAYOT
ATTN: L ROSSI
ATTN: P BENE
ATTN: S TAIMUTY

LTV AEROSPACE & DEFENSE COMPANY
ATTN: A.R. TOMME
ATTN: LIBRARY
ATTN: TECH DATA CENTER

MAGNAVOX ADVANCED PRODUCTS & SYS CO
ATTN: W HAGEMEIER

MARTIN MARIETTA CORP
ATTN: J TANKE
ATTN: J WARD
ATTN: MP-1601 W BRUCE
ATTN: R GAYNOR
ATTN: TIC/MP-30

MARTIN MARIETTA CORP
ATTN: T DAVIS

MARTIN MARIETTA DENVER AEROSPACE
ATTN: MS-D6074 M POLZELLA
ATTN: P KASE
ATTN: R ANDERSON
ATTN: RESEARCH LIBRARY

UNIVERSITY OF MARYLAND
ATTN: H C LIN

MCDONNELL DOUGLAS CORP
ATTN: A P MUNIE
ATTN: D L DOHM
ATTN: M STITCH
ATTN: R.L. KLOSTER

MCDONNELL DOUGLAS CORP
ATTN: D FITZGERALD
ATTN: P ALBRECHT

MCDONNELL DOUGLAS CORP
ATTN: TECH LIB

MESSENGER, GEORGE C
ATTN: G MESSENGER

MISSION RESEARCH CORP
ATTN: C LONGMIRE

MISSION RESEARCH CORP
ATTN: R PEASE

MISSION RESEARCH CORP
ATTN: J LUBELL
ATTN: R CURRY
ATTN: W WARE

MISSION RESEARCH CORP, SAN DIEGO
ATTN: J RAYMOND
ATTN: V VAN LINT

DEPT OF DEFENSE CONTRACTORS (CONTINUED)

MITRE CORP
ATTN: M FITZGERALD

MOTOROLA, INC
ATTN: A CHRISTENSEN

MOTOROLA, INC
ATTN: C LUND
ATTN: L CLARK
ATTN: O EDWARDS

NATIONAL SEMICONDUCTOR CORP
ATTN: F C JONES

UNIVERSITY OF NEW MEXICO
ATTN: DR NEAMEN

NORDEN SYSTEMS, INC
ATTN: N RIEDERMAN
ATTN: TECH LIB

NORTHROP CORP
ATTN: A BAHRAMAN
ATTN: J SROUR
ATTN: Z SHANFIELD

NORTHROP CORP
ATTN: E KING
ATTN: S STEWART

PACIFIC-SIERRA RESEARCH CORP
ATTN: H BRODE CHAIRMAN SAGE

PHYSICS INTERNATIONAL CO
ATTN: J SHEA

POWER CONVERSION TECHNOLOGY INC
ATTN: V FARGO

R & D ASSOCIATES
ATTN: P HAAS
ATTN: W KARZAS

RAND CORP
ATTN: C CRAIN
ATTN: P DAVIS
ATTN: B BENNETT

RAYTHEON CO
ATTN: G JOSHI
ATTN: J CICCIO

RAYTHEON CO
ATTN: A VAN DOREN
ATTN: H FLESCHER

RCA CORP
ATTN: G BRUCKER
ATTN: V MANCINO

RCA CORP
ATTN: R SMELTZER

RCA CORP
ATTN: R KILLION

RCA CORP
ATTN: E SCHMITT
ATTN: W ALLEN

RCA CORP
ATTN: E VAN KEUREN

RENSSELAER POLYTECHNIC INSTITUTE
ATTN: R GUTMANN
ATTN: R RYAN

RESEARCH TRIANGLE INSTITUTE
ATTN: M SIMONS

ROCKWELL INTERNATIONAL CORP
ATTN: A ROVELL
ATTN: GA50 TIC L G GREEN
ATTN: J BELL
ATTN: J BURSON
ATTN: K HULL
ATTN: V DE MARTINO
ATTN: V STRAHAN

ROCKWELL INTERNATIONAL CORP
ATTN: TIC AJ01

ROCKWELL INTERNATIONAL CORP
ATTN: L W PINKSTON
ATTN: TIC 124-203

ROCKWELL INTERNATIONAL CORP
ATTN: T YATES
ATTN: TIC BA08

SCIENCE APPLICATIONS INTL CORP
ATTN: D LONG
ATTN: D MILLWARD
ATTN: D STROBEL
ATTN: J NABER
ATTN: J SPRATT
ATTN: L SCOTT
ATTN: R FITZWILSON
ATTN: R J BEYSTER
ATTN: V ORPHAN
ATTN: V VERBINSKI

SCIENCE APPLICATIONS INTL CORP
ATTN: W CHADSEY

SCIENTIFIC RESEARCH ASSOC, INC
ATTN: H GRUBIN

SPERRY CORP
ATTN: J INDA

DEPT OF DEFENSE CONTRACTORS (CONTINUED)

SPERRY CORP
ATTN: P MARROFFINO

SPERRY CORP
ATTN: D SCHOW

SRI INTERNATIONAL
ATTN: A PADGETT

SUNDSTRAND CORP
ATTN: C WHITE

SYSTEM DEVELOPMENT CORP
ATTN: PRODUCT EVAL LAB

SYSTRON-DONNER CORP
ATTN: J RAY

TELEDYNE SYSTEMS CO
ATTN: R SUHRKE

TEXAS INSTRUMENTS, INC
ATTN: E JEFFREY MS 961
ATTN: F POBLENZ MS 3143
ATTN: J SALZMAN
ATTN: R MCGRATH
ATTN: T CHEEK MS 3143

TRW ELECTRONICS & DEFENSE SECTOR
ATTN: A WITTELES MS R1/2144
ATTN: D CLEMENT
ATTN: F FRIEDT
ATTN: H HOLLOWAY
ATTN: M S ASH
2 CYS ATTN: O ADAMS
ATTN: P GUILFOYLE
ATTN: P R REID
2 CYS ATTN: R PLEBUCH HARDNESS & SURV LAB
ATTN: R VON HATTEN
ATTN: TECH INFO CTR
ATTN: W B ADELMAN
ATTN: W ROWAN
ATTN: W WILLIS

TRW ELECTRONICS & DEFENSE SECTOR
ATTN: C BLASNEK
ATTN: F FAY
ATTN: J GORMAN

WESTINGHOUSE ELECTRIC CORP
ATTN: D GRIMES
ATTN: H KALAPACA
ATTN: R CRICCHI

WESTINGHOUSE ELECTRIC CORP
ATTN: S WOOD